Journal of Vibration Engineering & Technologies
https://doi.org/10.1007/s42417-022-00668-9

ORIGINAL PAPER

# Non-linear Isolator for Vibration and Force Transmission Control of Unbalanced Rotating Machines

**Loris Dal Bo[1] · Paolo Gardonio[1] · Nicola Battistella[1] · Emanuele Turco[1]**

Received: 24 September 2021 / Revised: 12 March 2022 / Accepted: 15 August 2022


## Abstract

**Purpose** The objective of this paper is to investigate with simulations how non-linear spring and non-linear damper components of isolators can be employed to effectively reduce both the oscillations and the force transmitted to ground in the whole spinning range of unbalanced rotating machines.

**Methods** The principal goal of this paper is twofold. First, to present a concise and consistent formulation based on the harmonic balance approach for the vibration response of spinning machines mounted on linear/non-linear, softening/hardening, un-tensioned/pre-tensioned springs and linear/non-linear dampers. Second, to provide a comprehensive overview of the vibration and force transmission control with non-linear isolators specifically tailored to unbalanced machines.

**Results** The study has shown that, the best vibration isolation is provided by a pre-tensioned linear and cubic softening spring combined with a linear and negative quadratic damper. The pre-tensioned spring should be designed in such a way as it holds the weight of the machine and thus produces on the vibrating machine a symmetric elastic restoring force proportional to the linear and cubic powers of the displacement. The cubic softening stiffness should then be tuned to minimise the frequency, and thus the amplitude, of the resonant response of the fundamental mode of the machine and elastic suspension system, while preserving stability and a desired static deflection. In parallel, to reduce the force transmission to ground above the fundamental resonance frequency, the negative quadratic damping effect should be tailored to maximize the energy absorption at higher frequencies.

**Conclusion** The study has shown that non-linear spring and non-linear damper components can be effectively employed to control the vibration and force transmission in the whole spinning range of the machine. In particular, a pre-tensioned softening cubic non-linear spring can be used to mitigate the vibration and force transmission at low frequencies, close to the fundamental natural frequencies of the elastically suspended machine. Also, a negative quadratic non-linear damper can be used to tailor the energy dissipation of the isolator in such a way as to have high damping at low frequencies and low damping at higher frequencies, which enhances the vibration and force transmission control at low frequencies and, rather importantly, mitigates the force transmission at higher frequencies.

**Keywords** Unbalanced spinning machines · Vibration isolation · Non-linear isolator · Cubic spring · Quadratic damper · Pre-tensioned spring

## Introduction

Vibration isolation is a challenging technical problem, which affects many types of mechanical systems, in particular those incorporating unbalanced rotating machines [1–5]. Indeed, rotating components can be found in several applications, including domestic appliances (e.g. washing machines, refrigerators), industrial plants (e.g. processing machineries, compressors, pumps), power plants (e.g. turbines, dynamos), surface vehicles (e.g. reciprocating engines, electric motors), air vehicles (e.g. turbo-fan engines, turbo-prop engines), etc.

✉ Paolo Gardonio
paolo.gardonio@uniud.it

Loris Dal Bo
dalbo.loris@spes.uniud.it

Nicola Battistella
battistella.nicola@spes.uniud.it

Emanuele Turco
turco.emanuele.1@spes.uniud.it

[1] Università degli Studi di Udine, DPIA, Via delle Scienze, 208-33100 Udine, Italy

Published online: 02 September 2022

[1]. Unbalance forces can result from the kinematics and the dynamics of the machines and from manufacturing and assembly imperfections of their components. Unbalance of fast rotating machines can generate significant centrifugal forces, which turn into large oscillations and large force transmission to ground [1–5]. To solve these problems, two types of remedies are normally employed: the first relies on balancing devices [6, 7] whereas the second is based on spring-damper isolators [8, 9]. The objective of this paper is to investigate with simulations how non-linear spring and non-linear damper components of isolators can be employed to effectively reduce both the oscillations and the force transmitted to ground in the whole spinning range of unbalanced rotating machines.

Vibration isolators are typically formed by spring-damper mounts, which connect the unbalanced rotating machine to the floor or to the housing structure [8]. Therefore, at low rotational velocities, i.e. at low frequencies, the vibration of the elastically suspended machine is affected by a cluster of resonances due to the fundamental natural modes characterised by linear and angular oscillations of the machine on the elastic mounts. In this way, the vibration of the machine is magnified at the low resonance frequencies and attenuated at higher frequencies to a value proportional to the ratio between the static unbalance (unbalance mass times the eccentricity) and the total mass of the elastically suspended machine [4]. The force transmission to the floor is also magnified at the low resonance frequencies. Moreover, at higher frequencies, it rises proportionally to frequency and can reach rather large values at the maximum spinning velocities [9]. To limit the vibration and force transmission resonance amplification effects, soft mounts should be employed, so that the cluster of resonances is shifted to very low frequencies, possibly outside the spinning range of the machine. However, this solution is normally restricted by static design constraints, which limit the static displacement of the suspended machine and thus the minimum allowed stiffness of the mounts. Both the vibration and force transmission resonance amplification phenomena as well as the higher frequencies large force transmission are linked to the damping produced by the mounts. For instance, a high damping effect tends to lower the vibration and force transmission at the resonance frequencies but also tends to enhance the force transmission at higher frequencies. Therefore, a trade-off solution is normally sought such that the mounts damping partially limits the vibration and force transmission at low frequencies and produces a somewhat small rise of force transmission at higher frequencies. In summary, to lower the vibration and force transmission in the whole spinning range of an unbalanced machine, the mounts should have high-static and small dynamic stiffness and should generate high damping at low frequencies and very small damping at higher frequencies [8]. These contrasting requirements cannot be fulfilled with classical isolators formed by linear spring and linear damper components. Therefore, compromising solutions are normally pursued, such that the low frequency vibration and force transmission amplification and the higher frequencies rise of force transmission are mitigated only in part.

To overcome these limitations, researchers have explored other solutions, such as active [10–13] or semi-active [14] isolators. Although these systems can, in principle, generate high vibration and ground force transmission control effects in the whole spinning range of the machine, their practical implementation has encountered a number of problems, linked primarily to fabrication, installation and maintenance costs, energy consumption to run the actuators and the controller as well as reliability concerns due to the complexity of the system.

During the past two decades, quite a few studies have been presented on non-linear passive isolators, which have shown how non-linear elastic and damping effects may significantly enhance the control performance of passive isolators. As pointed by Ho et al. [15], non-linear isolators can be classified in two groups. The first group uses hardening or softening non-linear springs [16, 17], which are commonly obtained from tilted axial springs [18–20]. The second group employs non-linear dampers, which tailor the spectrum of energy dissipation [21–24]. In general, non-linear spring and non-liner damper components offer concurrent solutions, particularly for the vibration isolation at low frequencies, where the response of the system is controlled by the cluster of resonances due to fundamental natural modes characterised by linear and angular oscillations of the machine. Therefore, the implementation of isolators equipped with both non-linear spring and non-linear damper components have been explored too. For instance, Ravindra and Mallik [25] investigated the vibration isolation effects produced by a suspension system formed by a non-linear spring characterised by a cubic hardening effect and by a non-linear damper chararacterised by Coulomb and viscous damping. Also, Ho et al. [15] studied the vibration isolation produced by a mount composed by a non-linear high-static and low-dynamic stiffness spring and a linear-cubic damper. Finally, Zhang et al. [26] investigated the effects of a cubic non-linear spring and cubic non-linear damper. Other types of non-linearities such as hard/soft springs combined with $n$-th power dampers were also investigated in Refs. [27–29]. Beside, non-linear isolators for high-static and low-dynamic stiffness were considered in Ref. [30], whereas two-stage non-linear isolators were investigated in Ref. [31]. A comprehensive review on non-linear passive vibration isolators can be found in Refs. [32–35].

Most of the studies on non-linear isolators considered machines excited by harmonic forces with constant amplitude, such that both the machine vibration and force

transmission are amplified at the resonance frequencies due to the fundamental natural modes of the elastically suspended machine and then effectively minimised at higher frequencies [15, 18, 24, 25, 29, 36]. Instead, this study is focussed on machines characterised by unbalanced spinning components, which produce large centrifugal forces, and thus large harmonic forces in vertical and transverse directions, proportional to the static unbalance and the squared angular velocity of the unbalanced rotating component. As a result, beside the vibration and force transmission amplification effects at the low resonance frequencies, at higher frequencies too there is a finite vibration level and a rise proportional to frequency of the force transmission, which are dictated by the machine unbalance and isolator damping respectively. The principal goal of this paper is thus twofold. First, to present a concise and consistent formulation for the vibration response of spinning machines mounted on linear/non-linear, softening/hardening, un-tensioned/pre-tensioned springs and linear/non-linear dampers. Second, to provide a comprehensive overview of the vibration and force transmission control with non-linear isolators specifically tailored to unbalanced machines.

The study investigates the vibration and force transmission in vertical direction of an unbalanced rotating machine, which is fixed to the base via a non-linear isolator. A simplified single-degree-of-freedom model problem is thus considered [3], which is characterised by a block mass and rotating unbalanced mass assembly connected to the floor via a spring and damper arranged in parallel. The free spring is characterised by a positive/negative cubic non-linearity whereas the damper is characterised by a negative quadratic non-linearity. Two configurations are considered where the spring is, or is not, pre-tensioned such that, when the spring is loaded by the weight of the machine, it produces respectively a symmetric elastic restoring force proportional to the linear and cubic powers of displacement [17, 25, 36] and an asymmetric elastic restoring force proportional to the linear, quadratic and cubic powers of displacement [37–40]. Both the effects of softening and hardening non-linear cubic springs are investigated. The vibration and force transmission produced by the unbalanced spinning machine mounted on the non-liner spring and non-linear damper is derived using the harmonic balance method [41–44]. The analysis is based on frequency spectra, which display the amplitude of the machine vibration and force transmission at the spinning velocity of the unbalanced mass. The study shows that the pre-tensioned softening non-linear spring can be effectively used to attenuate the machine vibration and force transmission in correspondence to resonance frequency due to the fundamental natural mode of the machine-mount system. Also, the non-linear negative quadratic damper [28] can be tailored in such a way as to generate the desired large damping effects at the resonance frequency and low damping effects at higher frequencies. As a result, significant machine vibration and force transmission control effects can be produced in the whole spinning range of the machine.

The paper is structured in four parts. "Isolator with Linear Spring and Linear Damper" section introduces the basic formulation for the equation of motion and force transmission to the floor of a machine mounted on a spring-damper isolator and briefly recalls the vibration isolation effects produced by a linear spring and a linear damper. "Isolator with Non-linear Spring and Linear Damper" section shows the vibration isolation effects produced by a pre-tensioned or un-tensioned, softening or hardening, cubic non-linear spring and linear damper. In parallel, "Isolator with Linear Spring and Non-linear Damper" section presents the vibration isolation effects generated by a linear spring and a negative quadratic non-linear damper. Finally, "Isolator with Non-linear Spring and Non-linear Damper" section shows the vibration isolation generated by a pre-tensioned softening cubic non-linear spring and a negative quadratic non-linear damper. Since the focus of the paper is on the effects produced by a non-linear isolator for vibration and force transmission control of spinning machines, to have a simple account, the details of the mathematical formulations used to derive the vibration and force transmission are reported in "Appendix A: Harmonic Balance Method" section. Also, the stability analysis for the systems with non-linear spring isolators is presented in "Appendix B: Equilibrium Points and Stability Analysis" section. Finally, "Appendix C: Forced Response to Harmonic Excitation: Steady-State Stability Analysis" section discusses the instability conditions such that the machine harmonic vibration swiftly jumps from low to high levels or, vice versa, from high to low levels.

## Isolator with Linear Spring and Linear Damper

This section briefly recalls the principal features that characterise the harmonic vibration and force transmission to ground in vertical direction of a spinning unbalanced machine mounted on a liner isolator. Also, it provides the core formulation for the analysis of all configurations involving linear and non-linear isolators. Therefore, the study considers the lumped parameter model shown in Fig. 1, where the physical properties of the lumped elements are summarised in Table 1. The analysis is based on a typical frequency domain formulation, although, to introduce the harmonic balance method employed in the following sections for the non-liner configurations, it is derived following a slightly different approach than usual. In fact, as discussed in "Appendix A: Harmonic Balance Method" section, the formulation assumes the harmonic excitation

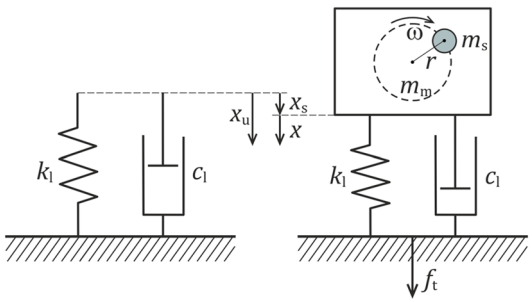


**Fig. 1** Lumped parameter model of the spinning unbalanced machine mounted on a linear spring and linear damper isolator

in vertical direction produced by the rotating unbalanced mass is characterised by an imposed frequency dependent phase lead, with equal amplitude to the phase lag generated by the response of the system at each frequency. In this way, the response of the system can be expressed in terms of an harmonic function with no phase delay. This mathematical artefact greatly simplifies the harmonic balance formulation used to solve the non-linear equations of motion for the machine mounted on non-linear isolators [27]. For simplicity, the frequency dependence of the amplitude functions for the machine displacement and transmitted force have been omitted in the intermediate steps of the formulations presented below and in the following sections.

According to Fig. 1, the model is formed by a block mass $m_m$ and an unbalance rotating mass $m_s$ assembly, which is mounted on an isolator composed by a linear spring $k_l$ and linear viscous damper $c_l$. The unbalance mass rotates with constant angular speed $\omega$ along a circumference of radius $r$. Therefore, the block mass $m_m$ is excited in vertical direction by an harmonic force proportional to the unbalance mass, the radius and the spinning velocity squared, i.e. $m_s r\omega^2$. The equation of motion for the vertical displacement is derived applying Newton's second law of motion, which gives

$$m\ddot{x}(t) = -f_k(t) - f_c(t) + mg + m_s r\omega^2 \sin(\omega t + \theta(\omega)), \quad (1)$$

where $m = m_m + m_s$ is the aggregate mass of the machine, $m_m$, and unbalance mass, $m_s$, which rotates with constant angular velocity $\omega$ and offset $r$. Also, $f_k(t)$ and $f_c(t)$ are the forces generated by the linear spring and linear damper elements, which are depicted by the black lines in Fig. 2.

As anticipated above, to be consistent with the formulations presented in the following sections for the machine mounted on non-linear isolators, the harmonic excitation produced by the spinning unbalance mass is defined with respect to a phase lead $\theta(\omega)$, equal to the phase delay that would characterise the harmonic vibration of the machine

**Table 1** Physical properties of the machine and isolators

| Configurations | Property | Value |
|---|---|---|
| All | Machine mass | $m_m = 60\text{kg}$ |
| | Unbalanced rotating mass | $m_s = 4\text{kg}$ |
| | Machine total mass | $m = 64\text{kg}$ |
| Linear isolator ("Isolator with Linear Spring and Linear Damper" section) | Linear stiffness | $k_l = 22739\text{N/m}$ |
| | Linear damping | $c_l = 500\text{Ns/m}$ |
| | Fundamental natural frequency | $f_l = 3\text{Hz}$ |
| | Damping ratio | $\xi_l = 0.21$ |
| Pre-tensioned non-linear spring and linear damper isolator ("Isolator with a Pre-tensioned Spring" section) | Softening cubic non-linear stiffness | $k_1 = 22739\text{N/m}$, $k_3 = -97.2, -194.5, -396.8 \times 10^5\text{N/m}^3$ |
| | Hardening cubic non-linear stiffness | $k_1 = 22739\text{N/m}, k_3 = 26.88, 67.2 \times 10^5\text{N/m}^3$ |
| | Linear damping | $c_1 = 500\text{Ns/m}$ |
| Un-tensioned non-linear spring and linear damper isolator ("Isolator with an Un-tensioned Spring" section) | Softening quadratic and cubic non-linear stiffness | $\widetilde{k}_1 = 30762\text{N/m}, k_1 = 21719\text{N/m}$, $k_2 = -4 \times 10^5\text{N/m}^2\, k_3 = -60.8 \times 10^5\text{N/m}^3$ |
| | Linear damping factor | $c_1 = 500\text{Ns/m}$ |
| Linear spring and non-linear damper isolator ("Isolator with Linear Spring and Non-linear Damper" section) | Linear stiffness | $k_1 = 22739\text{N/m}$ |
| | Quadratic non-linear damping | $c_1 = 500\text{Ns/m}, c_2 = -64, -90\text{Ns}^2/\text{m}^2$ |
| Pre-tensioned non-linear spring and non-linear damper isolator ("Non-linear Isolator with a Pre-tensioned Non-linear Spring and a Non-linear Damper" section) | Softening cubic non-linear stiffness | $k_1 = 22739\text{N/m}, k_3 = -291.8 \times 10^5\text{N/m}^3$ |
| | Quadratic non-linear damping | $c_1 = 830\text{Ns/m}, c_2 = -246\text{Ns}^2/\text{m}^2$ |
| Un-tensioned non-linear spring and non-linear damper isolator ("Non-linear Isolator with an Un-tensioned Spring" section) | Softening quadratic and cubic non-linear stiffness | $\widetilde{k}_1 = 30762\text{N/m}, k_1 = 21719\text{N/m}$, $k_2 = -4 \times 10^5\text{N/m}^2$, $k_3 = -60.8 \times 10^5\text{N/m}^3$ |
| | Quadratic non-linear damping | $c_1 = 768\text{Ns/m}, c_2 = -224\text{Ns}^2/\text{m}^2$ |

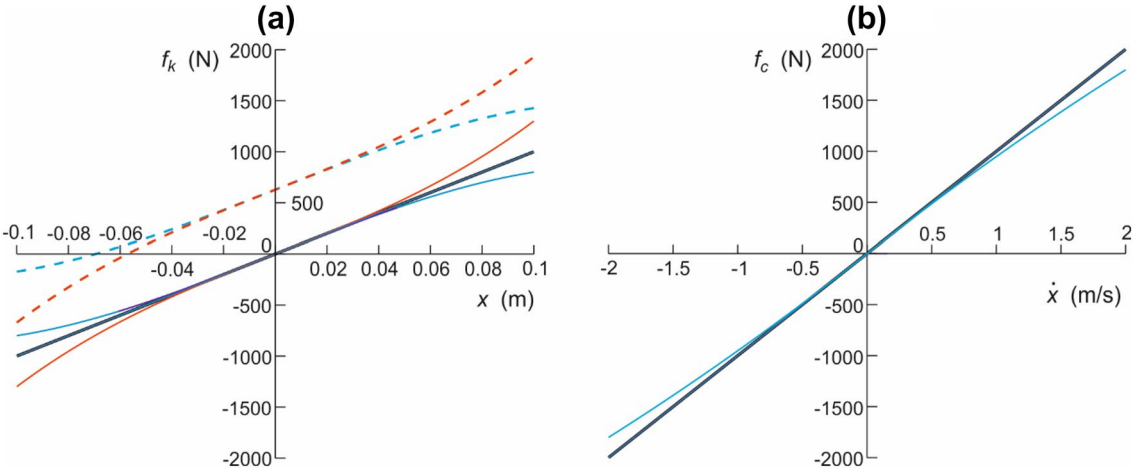


**Fig. 2** **a** Elastic force of the linear (solid black line), non-linear untensioned softening (solid blue line) and hardening (solid red line), non-linear pre-tensioned softening (dashed blue line) and hardening (dashed red line) springs. **b** Dissipative force of the linear (solid black line) and non-linear (solid blue line) dampers. To better visualise the non-linear effects, the two graphs consider rather wide displacement and velocity ranges (colour figure online)

at each frequency. Accordingly, the response is bound to be given by an harmonic function with no phase delay [27]. The constitutive equations for the linear spring and linear damper, are given by:

$$f_k(t) = k_l x_u(t), \tag{2}$$

$$f_c(t) = c_l \dot{x}(t), \tag{3}$$

where $k_l$ and $c_l$ are the stiffness and damping coefficients of the linear isolator given in Table 1. Also,

$$x_u(t) = x_s + x(t), \tag{4}$$

is the displacement with respect to the unloaded isolator top end and, $x(t)$ is the displacement with respect to the loaded isolator top end and $x_s = mg/k_l$ is the static displacement of the isolator produced by the weight of the machine ($g = 9.81\text{m/s}^2$ is the standard acceleration of gravity). Therefore, substituting Eqs. (2), (3), (4) into Eq. (1), the equation of motion can be rewritten in the following canonical form:

$$m\ddot{x}(t) + c_l\dot{x}(t) + k_l x(t) = m_s r\omega^2 \sin(\omega t + \theta(\omega)). \tag{5}$$

Assuming the harmonic vibration of the machine is given in the form

$$x(t) = X \sin(\omega t), \tag{6}$$

after some mathematical manipulations, the following algebraic equation is derived with respect to the amplitude of the machine harmonic vibration $X(\omega)$:

$$\left(-m\omega^2 + k_{1l}\right)^2 X^2 + c_{1l}^2\omega^2 X^2 = m_s^2 r^2 \omega^4. \tag{7}$$

Accordingly, the amplitude of the machine harmonic vibration results:

$$X(\omega) = \frac{\frac{\omega^2}{\omega_l^2} e}{\sqrt{\left(1 - \frac{\omega^2}{\omega_l^2}\right)^2 + \left(2\xi_1 \frac{\omega}{\omega_l}\right)^2}}, \tag{8}$$

where $\omega_l = \sqrt{k_l/m}$ is the natural frequency, $\xi_l = c_l/(2\omega_l m)$ is the damping ratio and $e = m_s r/m$ is the specific unbalance [7]. This expression suggests that the amplitude of the machine vibration, is characterised by the typical spectrum of a second order system multiplied by $\omega^2$.

As can be deduced directly from the lumped parameter model shown in Fig. 1, the force transmitted to ground is given by:

$$f_t(t) = f_k(t) + f_c(t), \tag{9}$$

such that, using Eqs. (2), (3) and neglecting the load produced by the weight of the machine,

$$f_t(t) = k_l x(t) + c_l \dot{x}(t). \tag{10}$$

Since for time-harmonic vibrations the machine displacement and velocity are in quadrature, the harmonic forces transmitted to the floor by the spring and damper are also 90° out of phase. Hence, the amplitude of the time-harmonic total force transmitted to the floor can be written as follows:

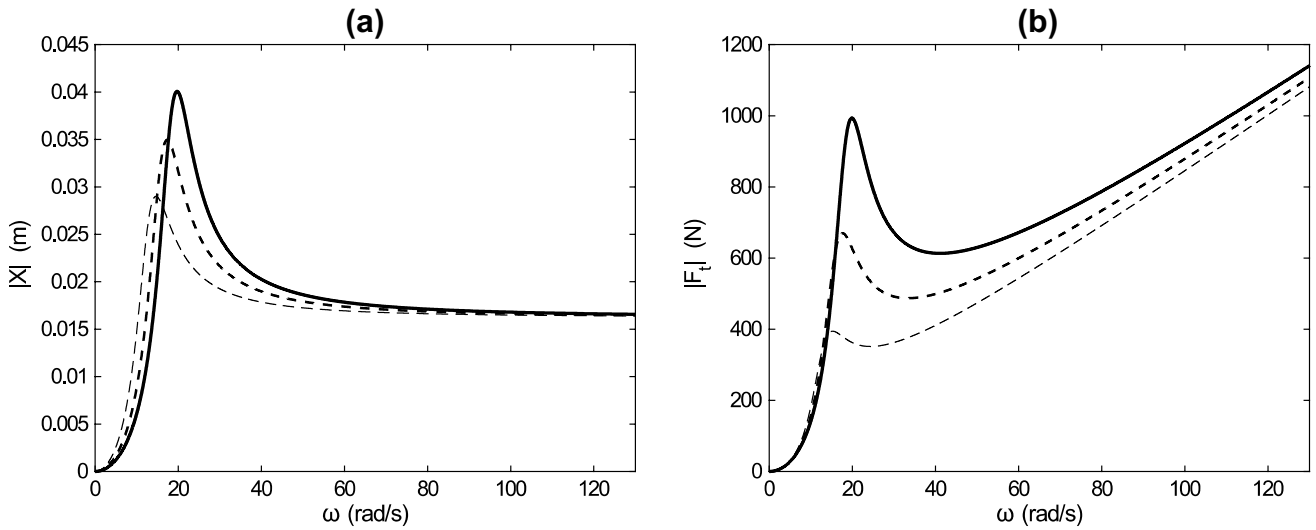


**Fig. 3** Spectra of the vibration **a** and force transmission **b** amplitudes of the machine mounted on the reference spring-damper linear isolator (thick solid lines) and on linear isolators with progressively softer springs (dashed lines)

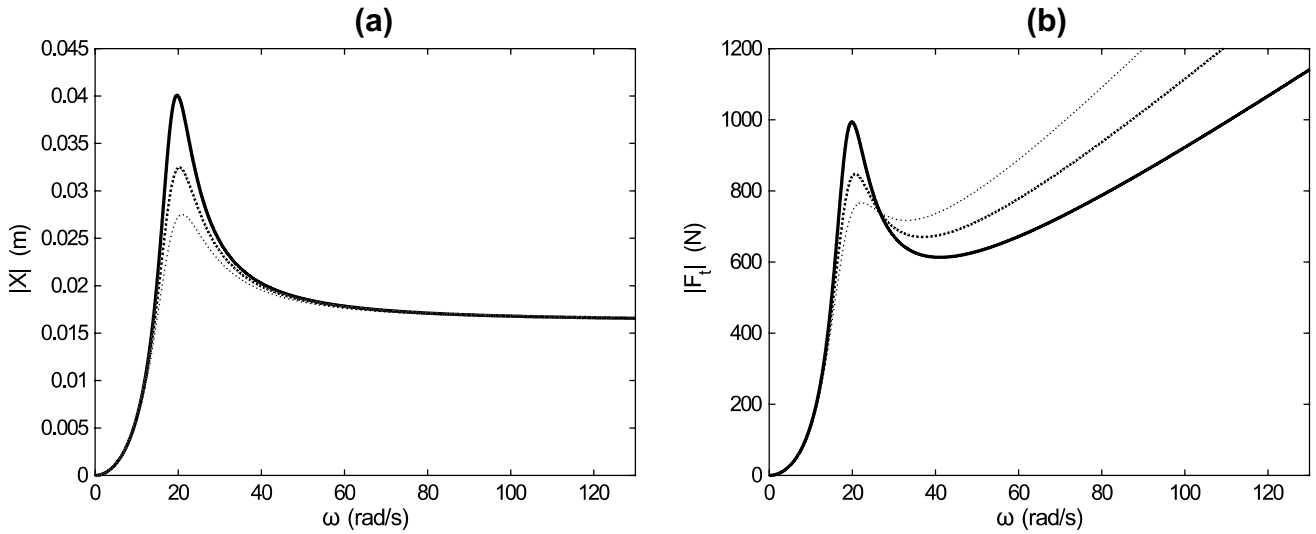


**Fig. 4** Spectra of the vibration **a** and force transmission **b** amplitudes of the machine mounted on the reference linear spring-damper isolator (thick solid lines) and on linear isolators with progressively larger dampers (dotted lines)

$$F_t(\omega) = \sqrt{k_l^2 + c_l^2\omega^2}X(\omega) = c_l\omega\sqrt{1 + \frac{k_l^2}{c_l^2\omega^2}}X(\omega). \qquad (11)$$

This expression suggests that the amplitude of the force transmitted to ground is proportional to the machine vibration amplitude $X(\omega)$ and to the machine angular velocity $\omega$, that is, to the frequency of the harmonic excitation in vertical direction exerted by the rotating unbalance mass. Therefore it should replicate the features of the spectrum of the machine vibration amplitude multiplied by $\omega$.

Figures 3 and 4 show the spectra for the vibration and force transmission amplitudes of the machine mounted on the reference spring-damper isolator (thick solid black lines) and on isolators with progressively softer springs (dashed black lines in Fig. 3) and progressively larger dampers (dotted black lines in Fig. 4). Considering first the spectra for the vibration amplitude of the machine mounted on the reference spring-damper isolator, the thick-solid black lines in Plots (a) show the typical spectrum characterised by a marked peak at about the fundamental natural frequency of the machine-isolator system and then a constant level at higher frequencies. For lightly damped

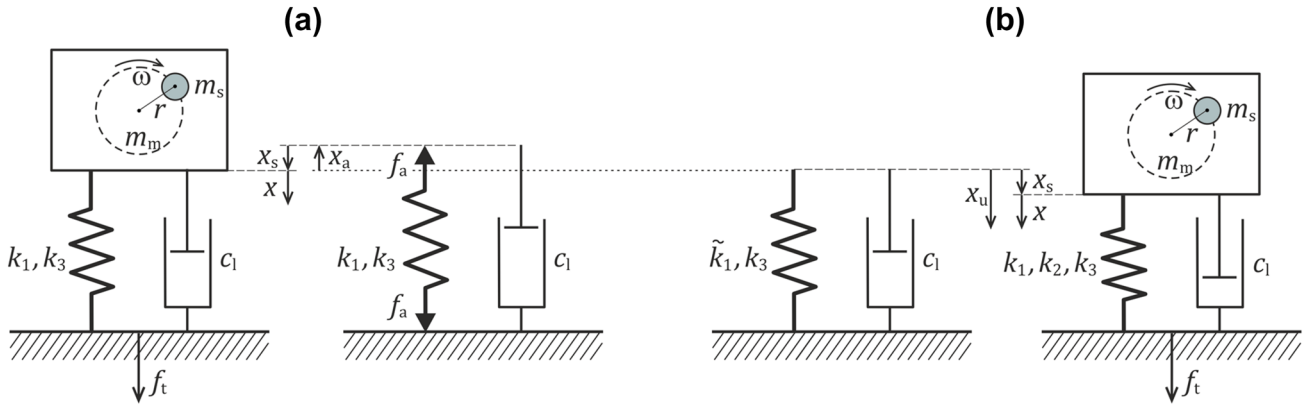


**Fig. 5** Lumped parameter model of the spinning unbalanced machine mounted on pre-tensioned **a** and un-tensioned **b** cubic non-linear spring and linear damper isolator

isolators, the peak amplitude can be derived from Eq. (8) after setting $\omega = \omega_l$:

$$X_{mx} \cong X(\omega_l) = \frac{m_s r}{c_l}\omega_l = \frac{e}{2\xi_l}. \tag{12}$$

Also, at higher frequencies such that $\omega \gg \omega_l$, according to Eq. (8), the amplitude of the machine vibration asymptotically tends to a constant value given by:

$$X(\omega >> \omega_l) \cong e, \tag{13}$$

where here and in the previous equation $e = m_s r/m$ is the specific unbalance. Equation (12) indicates that the peak amplitude can be reduced either by lowering the natural frequency of the machine-isolator system, $\omega_l$, or by increasing the damping of the isolator, $c_l$. Indeed, as can be noticed in plots (a) of Figs. 3 and 4, the peak amplitude tends to decrease as the isolator stiffness is lowered or, alternatively, as the isolator damping $c_l$ is raised. Equation (13) shows that the constant amplitude asymptote for large frequencies is given by the specific unbalance $e = m_s r/m$. Thus, it depends on the properties of the unbalanced machine rather than those of the isolator. Indeed, Plots (a) of Figs. 3 and 4 show that neither the stiffness nor the damping of the isolator influence the amplitude of the machine oscillation at frequencies greater than the fundamental natural frequency of the machine-mount system.

Considering now the spectra for the amplitude of the force transmitted to the floor when the machine is mounted on the reference spring-damper isolator, the thick-solid black lines in Plots (b) show the classical spectrum characterised by a marked peak at about the fundamental natural frequency of the machine-isolator system and then, at higher frequencies, a constant raise proportional to frequency. For lightly damped isolators, the peak amplitude can be derived from Eq. (11) after setting $\omega = \omega_l$:

$$F_{t,mx} = k_l\sqrt{1+4\xi_l^2}X_{mx} \cong k_l\sqrt{1+\frac{1}{4\xi_l^2}}e. \tag{14}$$

At higher frequencies than the fundamental natural frequency, the second term in the square root of Eq. (11) prevails, so that the amplitude of the transmitted force can be approximated with the following expression:

$$F_t(\omega > \omega_l) \cong \omega c_l X(\omega > \omega_l) \cong \omega c_l e. \tag{15}$$

As found for the vibration amplitude, Eqs. (14) and (15) encompass the specific unbalance $e = m_s r/m$. Also, as found for the machine vibration, Eq. (14) suggests that the peak amplitude of the force transmitted to the floor can be reduced either by lowering the natural frequency of the machine-isolator system, $\omega_l$, or by increasing the damping of the isolator, $c_l$. This is confirmed by Plots (b) of Figs. 3 and 4, which show significant reductions of the peak force transmission both when the isolator stiffness is lowered and when the isolator damping $c_l$ is raised. Also, Eq. (15) indicates that, for larger frequencies than the fundamental natural frequency, the force transmitted to the floor raises proportionally to the frequency, to the isolator damping and to the unbalance eccentricity. Therefore, as can be noticed from Plots (b) of Figs. 3 and 4, for $\omega > \omega_l$, the force transmission to the floor can be lowered by decreasing the damping effect of the mount. Instead, the stiffness of the isolator does not influence the force transmission at higher frequencies.

In summary, from this short overview, it can be concluded that, to guarantee a high vibration isolation effect, the suspension should be characterised by a soft dynamic stiffness, although it should also provide a large static stiffness to

guarantee a small static displacement. Moreover, the damping effect should be tailored in such a way as to generate high damping at low frequencies around the fundamental natural frequency of the machine-suspension system and very low damping at higher frequencies so as to guarantee significant vibration control performance both at low and high frequencies. These requirements can be satisfied only partially with linear spring–damper isolators. Therefore, the following three sections investigate how these effects can be generated by isolators encompassing a non-linear spring and a non-linear damper.

## Isolator with Non-linear Spring and Linear Damper

The effects produced by a suspension with a non-linear spring are first examined in this section. The analysis is thus based on the lumped parameter models shown in Fig. 5, where the physical properties of the lumped elements are summarised in Table 1. Two cases are considered, where, as shown in Fig. 2a, the spring is either pre-tensioned (dashed blue and red lines) or un-tensioned (solid blue and red lines). In the first case, the spring is pre-loaded with a tensioning axial force equal to the weight of the machine and unbalance mass, that is

$$f_a = mg. \tag{16}$$

Therefore, as shown below, when the suspension is loaded by the weight of the machine and unbalance mass, the tensioned non-linear spring produces a symmetric elastic restoring force on the machine and rotating mass proportional to the displacement and to the cube of the displacement of the suspended machine. Alternatively, the un-tensioned spring, generates an asymmetric elastic restoring force proportional to the displacement, to the square of the displacement and to the cube of the displacement of the suspended machine. As discussed in "Appendix B: Equilibrium Points and Stability Analysis" section, a softening cubic non-linear springs may lead to an unstable machine-isolator system. Therefore, the coefficients for the softening cubic spring considered in this study were selected in a range that guarantees stability.

### Isolator with a Pre-tensioned Spring

The vibration and force transmission when, as shown in Fig. 5a, the machine is mounted on pre-tensioned softening and hardening cubic non-linear spring (dashed blue and red lines in Fig. 2a) is first investigated here. In this case, the constitutive equation for the pre-tensioned non-linear spring is given by [25, 26, 28]:

$$f_k(t) = k_1 x(t) + k_3 x^3(t) + f_a, \tag{17}$$

where $k_1$, $k_3$ are the coefficients for the linear and cubic stiffness effects. For the softening non-linear spring $k_3 < 0$ whereas for the hardening cubic spring $k_3 > 0$. Therefore, using Eqs. (17) and (3) into Eq. (1), the equation of motion results

$$m\ddot{x}(t) + c_l\dot{x}(t) + k_1 x(t) + k_3 x^3(t) = m_s r\omega^2 \sin(\omega t + \theta(\omega)). \tag{18}$$

As discussed in "Appendix A: Harmonic Balance Method" section, the steady-state periodic vibration of the machine is derived using the harmonic balance method [41–45], which assumes the periodic response is approximated by a Fourier series and considers only the fundamental component of the series, such that

$$x(t) = X_1 \sin(\omega t). \tag{19}$$

Therefore, substituting Eq. (19) into Eq. (18), after some mathematical manipulations and neglecting the higher harmonic term in $\sin(3\omega t)$, the following algebraic equation is derived with respect to $X_1$ and ω:

$$\left(-m\omega^2 + k_1 + \frac{3}{4}k_3 X_1^2\right)^2 X_1^2 + c_1^2\omega^2 X_1^2 = m_s^2 r^2 \omega^4. \tag{20}$$

Unlike the classical approach used for linear systems, here, the values of $\omega$ satisfying Eq. (20) are sought numerically with reference to a range of amplitudes $X_1$ that guarantee real positive solutions, i.e. $\omega > 0$. Overall, the resulting function $X_1(\omega)$ is not uniquely defined with respect to $\omega$ since for certain frequencies three values of $X_1(\omega)$ may satisfy Eq. (20). This leads to the typical spectrum of $X_1(\omega)$ with two branches for a given frequency, such that the resonance peak is tilted either to the left hand side or to the right hand side of $\omega_l$, respectively for softening and hardening non-linear springs [41–43]. As discussed in "Appendix C: Forced Response to Harmonic Excitation: Steady-State Stability Analysis" section, this phenomenon can be regarded as an instability of the steady state motion [43], where the amplitude of the machine vibration swiftly jumps from the upper branch to the lower branch or vice versa, depending whether the spinning machine is speeding up or slowing down.

In this case, recalling Eq. (9), the force transmitted to the floor results given by:

$$f_t(t) = k_1 x(t) + k_3 x^3(t) + c_l\dot{x}(t). \tag{21}$$

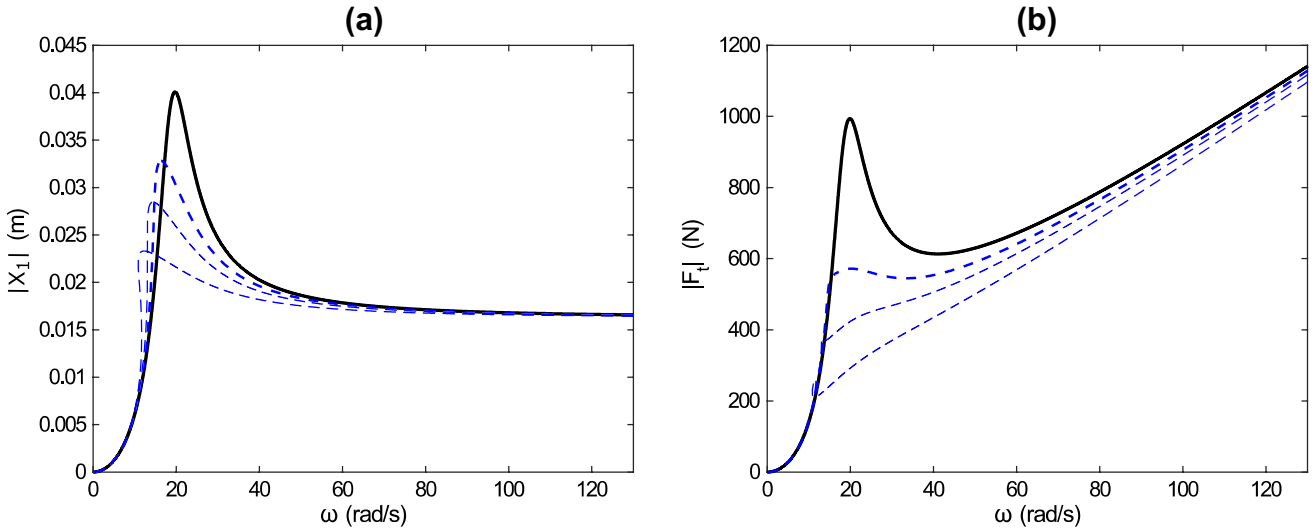


**Fig. 6** Spectra of the vibration **a** and force transmission **b** amplitudes of the machine mounted on the reference linear spring-damper isolator (thick solid black lines) and on pre-tensioned non-linear isolators with progressively softening cubic springs (dashed blue lines) (colour figure online)

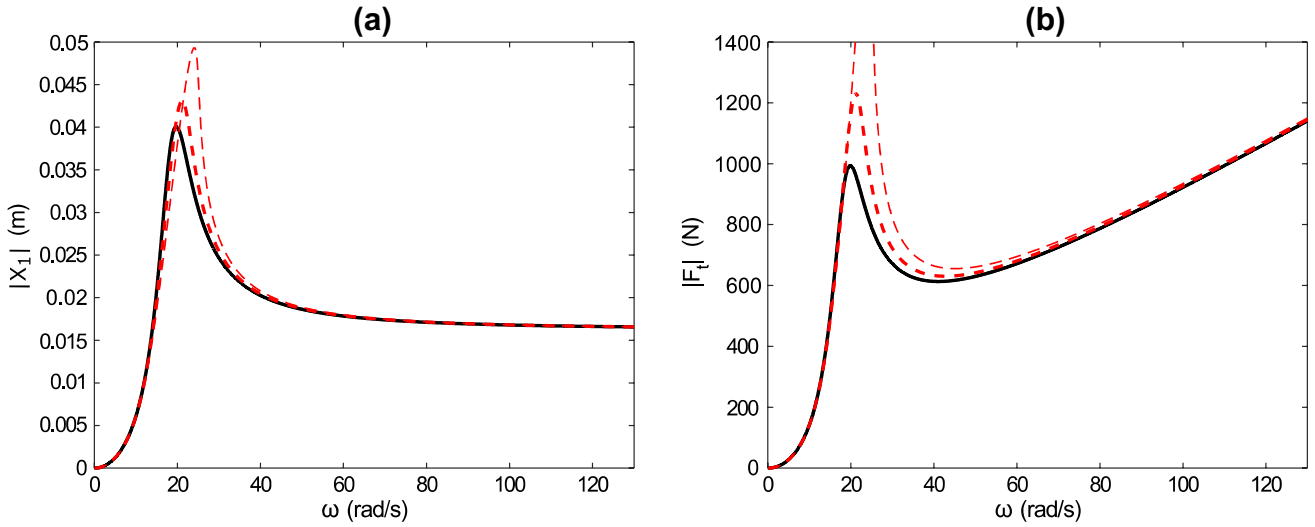


**Fig. 7** Spectra of the vibration **a** and force transmission **b** amplitudes of the machine mounted on the reference linear spring-damper isolator (thick solid black lines) and on pre-tensioned non-linear isolators with progressively hardening cubic springs (dashed red lines) (colour figure online)

Therefore, using Eq. (19) with $X_1(\omega)$ derived numerically from Eq. (20) and remembering that for time-harmonic vibrations of the machine, the harmonic forces transmitted to the floor by the spring and damper are 90° out of phase, the amplitude of the force transmitted to ground results given by:

$$\begin{aligned} F_t(\omega) &= \sqrt{\left(k_1 X_1 + \frac{3}{4}k_3 X_1^3(\omega)\right)^2 + c_1^2\omega^2 X_1^2} \\ &= c_l\omega\sqrt{1+\left(\frac{k_1}{c_1\omega}+\frac{3}{4}\frac{k_3}{c_1\omega}X_1^2\right)^2}X_1. \end{aligned} \tag{22}$$

As seen for the linear isolator, this expression suggests that the force transmitted to ground depends on the machine vibration amplitude $X_1(\omega)$ and to the angular frequency $\omega$ of the harmonic excitation exerted by the rotating unbalance

mass. Moreover, at low frequencies where the stiffness effect is comparatively larger than the damping effect, a softening non-linear spring with $k_3 < 0$ tends to reduce the force transmission, whereas a hardening non-linear spring with $k_3 > 0$ tends to increase the force transmission.

Figures 6 and 7 show the spectra for the vibration (Plots a) and force transmission (Plots b) amplitudes of the machine mounted on the reference linear spring-damper linear isolator (thick solid black lines) and on isolators with progressively softening and progressively hardening (dashed blue lines in Fig. 6, dashed red lines in Fig. 7, respectively) non-linear springs. To provide a fair comparison with the results presented for the machine mounted on the reference linear isolator, the linear coefficient for the spring has been set such that $k_1 = k_l$. Also, the values reported in Table 1 have been adopted for the cubic coefficients of the softening ($k_3 < 0$) and hardening ($k_3 > 0$) non-linear springs. The dashed blue lines in Plot a of Fig. 6 indicate that, as the softening effect produced by the negative cubic term (i.e. $k_3 < 0$) of the non-linear spring is raised, the resonance peak is progressively lowered and bent to the left hand side such that the resonance frequency is shifted to lower values. Accordingly, below $\omega_1 = \sqrt{k_1/m}$, the spectrum progressively shows a frequency region with a double branch. Here the response is typically unstable and characterised by the so-called "jump phenomenon" [45–48], where indeed the machine vibration swiftly pops from low to high or from high to low amplitudes depending whether the rotating machine is speeding-up or slowing-down, respectively. In contrast, the dashed red lines in Plot a of Fig. 7 suggest that a hardening non-linear spring would bend the resonance peak to the right hand side so that the double-branch unstable region occurs in a frequency band just above $\omega_1 = \sqrt{k_1/m}$. In this case, the hardening effect produced by the positive cubic term (i.e. $k_3 > 0$) of the non-linear spring tends to increase the resonance frequency and the amplitude of the peak response. These effects can be readily quantified considering the peak response of the machine vibration for a lightly damped suspension. As shown in Appendix "Machine Mounted on the Non-linear Pre-tensioned Isolator" section, assuming light damping such that $\xi_1^2 \ll 0.5$, it is possible to obtain the following approximate analytical solution for the peak response:

$$X_{1,mx} \cong \frac{\omega_1}{\sqrt{\left(\frac{c_l}{m_s r}\right)^2 - \frac{3}{4}\frac{k_3}{m}}} = \frac{\omega_1}{\sqrt{\left(\frac{2\xi_1\omega_1}{e}\right)^2 - \frac{3}{4}\beta_3}}, \tag{23}$$

where $\omega_1 = \sqrt{k_1/m}$, $\xi_1 = c_l/(2\omega_1 m)$, $e = m_s r/m$ and $\beta_3 = k_3/m$ (setting $k_3 = 0$ Eq. (23) reduces to Eq. (12)). Indeed, this expression suggests that a softening cubic spring ($k_3 < 0$) would lower the amplitude of the peak response at the resonance frequency whereas a hardening cubic spring ($k_3 > 0$) would increase it.

The spectra in Plots b of Figs. 6 and 7 show somehow similar features for the amplitude of the force transmitted to the floor via the non-linear isolator with softening and hardening non-linear springs, respectively. However, the spectrum for the isolator with the softening spring in Plot b of Fig. 6 shows only a very small deviation of the resonance peak to the left hand side. The resonance peak is actually quite similar to that obtained for the machine mounted on the linear isolator shown in Fig. 3b. Alternatively, the spectrum for the isolator with the hardening spring in Plot b of Fig. 7 shows a striking right hand side deviation and rise of the resonance peak. These effects can be readily explained considering the peak force transmission for a lightly damped suspension. In this case, assuming $\xi_1^2 \ll 0.5$ and $\omega = \omega_1$, Eq. (22) becomes

$$F_{t1,mx} \cong c_l\omega_1\sqrt{1 + \left(\frac{k_1}{c_l\omega_1} + \frac{3}{4}\frac{k_3}{c_l\omega_1}X_{1,mx}^2\right)^2}\,X_{1,mx}. \tag{24}$$

This expression confirms that a softening effect of the non-linear spring such that $k_3 < 0$ tends to lower the peak force transmission whereas the hardening effect such that $k_3 > 0$ brings up the peak force transmission.

## Isolator with an Un-tensioned Spring

The vibration and force transmission when, as shown in Fig. 5b, the machine is mounted on an un-tensioned non-linear spring (solid blue and red lines in Fig. 2a) is now investigated. Based on the results presented above, only the effect of a softening non-linear spring is considered, which guarantees a reduction of the response and force transmission at resonance frequency. In this case, the constitutive equation for the un-tensioned cubic non-linear spring is given by [25, 26, 28]:

$$f_k(x_u, t) = \tilde{k}_1 x_u(t) + k_3 x_u^3(t), \tag{25}$$

where $\tilde{k}_1$ and $k_3$ are the linear and cubic stiffness coefficients. In this case, substituting Eqs. (25) and (3) into Eq. (1), the equation of motion results given by:

$$\begin{aligned} &m\ddot{x}(t) + c_l\dot{x}(t) + k_1 x(t) k_2 x(t)^2 + k_3 x(t)^3 \\ &= m_s r\omega^2 \sin(\omega t + \theta(\omega)). \end{aligned} \tag{26}$$

where $k_1$ and $k_2$ are given by:

$$k_1 = \tilde{k}_1 + 3k_3 x_{st}^2, \tag{27}$$

$$k_2 = 3k_3 x_{st}. \tag{28}$$

As can be deduced from Eqs. (27), (28), under the static weight of the machine, the non-linear elastic restoring force becomes asymmetric and characterised by an additional

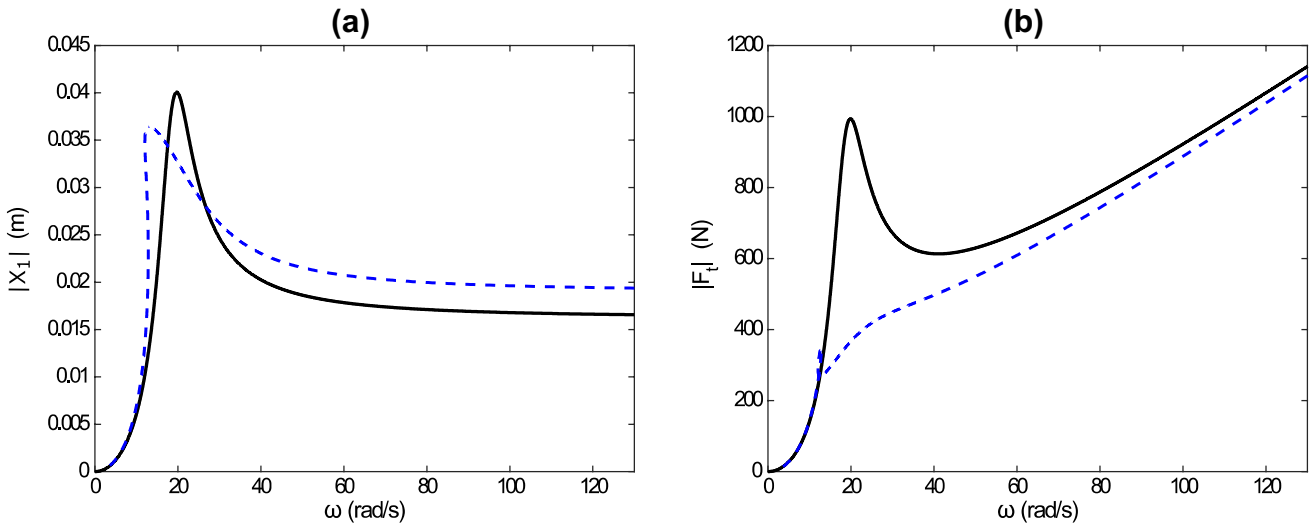


**Fig. 8** Spectra of the vibration **a** and force transmission **b** amplitudes of the machine mounted on the reference linear spring-damper isolator (thick solid black lines) and on an un-tensioned non-linear isolator with softening cubic spring (thick dashed blue lines) (colour figure online)

negative quadratic term $k_2$. Also, the linear stiffness term is reduced by the factor $3k_3x_{st}^2 < 0$. As discussed in "Appendix A: Harmonic Balance Method" section, with the harmonic balance method the periodic response of the machine non-linear system governed by Eq. (26) is given by the fundamental component of the Fourier series that approximates the periodic response of the machine, such that [37–40]:

$$x(t) = X_0 + X_1 \sin(\omega t), \tag{29}$$

where $X_0$ represents the off-set around which the machine oscillates at each excitation frequency $\omega$ with respect to the unloaded spring. Substituting Eq. (29) into Eq. (26), the following two algebraic equations are derived with respect to the amplitude of the machine harmonic vibration $X_1$, where higher order harmonic terms of the type $\sin(3\omega t)$, $\cos(3\omega t)$, $\cos(2\omega t)$, are neglected:

$$\left(\left(-m\omega^2 + k_1 + 2k_2X_0 + 3k_3X_0^2\right)X_1 + \frac{3}{4}k_3X_1^3\right)^2 + c_l^2\omega^2X_1^2 = m_s^2r^2\omega^4, \tag{30}$$

$$k_3X_0^3 + k_2X_0^2 + \left(k_1 + \frac{3}{2}k_3X_1^2\right)X_0 + \frac{1}{2}k_2X_1^2 = 0. \tag{31}$$

Here, the value of $X_1$ is first derived from Eq. (31) with respect to the amplitudes of $X_0$. Equation (30) is then solved with the same numerical approach as that employed for Eq. (20).

Recalling Eq. (9) and neglecting the effect produced by the weight of the machine, the force transmitted to ground is given by:

$$f_t(t) = k_1x(t) + k_2x^2(t) + k_3x^3(t) + c_l\dot{x}(t). \tag{32}$$

Therefore, considering Eq. (29) with $X_0(\omega), X_1(\omega)$ derived from Eqs. (30), (31) and recalling that for time-harmonic vibrations of the machine, the harmonic forces transmitted to the floor by the spring and damper are 90° out of phase, the amplitude of the force transmitted to ground results given by:

$$F_t(\omega) = \left(k_1X_0 + k_2X_0^2 + k_3X_0^3 + \frac{1}{2}\left(3k_3X_0 + k_2\right)X_1^2\right) + \sqrt{\left(k_1X_1 + \frac{3}{4}k_3X_1^3 + 3k_3X_0^2X_1 + 2k_2X_0X_1\right)^2 + \left(c_l\omega X_1\right)^2} \tag{33}$$

Compared to Eq. (22), this is a rather involved expression, which, nonetheless, indicates that the force transmitted to ground depends on the offset $X_0$ and amplitude $X_1(\omega)$ of the machine vibration and on the angular frequency $\omega$ of the harmonic excitation exerted by the rotating unbalance mass. Moreover, at low frequencies where the stiffness effect is comparatively larger than the damping effect, the softening effects generated by the intrinsic properties of the non-linear spring (i.e. $k_3 < 0$) and by the loading effect (i.e. $k_2 < 0$) tend to further reduce the force transmission.

Figure 8 shows the spectra for the vibration (Plots a) and force transmission (Plots b) amplitudes of the machine mounted on the reference spring-damper linear isolator (thick solid black lines) and on the isolator with the un-tensioned softening non-linear spring (thick dashed blue lines). Also in this case, to have a fair comparison with the results presented for the machine mounted on the reference linear isolator, the linear and non-linear stiffness terms $\widetilde{k}_1$ and $k_3$ reported in Table 1 have been chosen in such a way as the static deflection $x_{st}$ is comparable to that of the machine mounted on the linear spring, that is $x_{st} = \frac{mg}{k_l}$. These

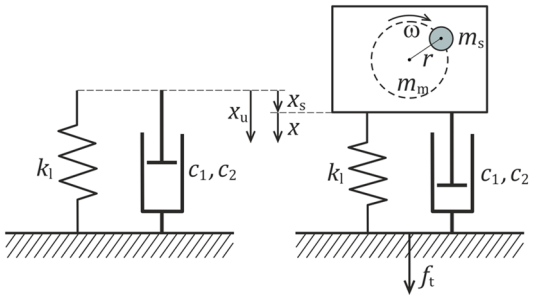


**Fig. 9** Lumped parameter model of the spinning unbalanced machine mounted on a linear spring and a negative quadratic non-linear damper isolator

values guarantee the maximum amplitude of oscillation is sufficiently far from the unstable equilibrium point too. The thick dashed blue line in Plot a of Fig. 8 indicates that, as found for the pre-tensioned non-linear spring, the softening effect produced by the negative cubic term (i.e. $k_3 < 0$) bends the resonance peak to the left hand side such that the resonance frequency is significantly lowered. Moreover, it tends to lower the amplitude of the peak response, although, compared to the isolator with the pre-tensioned spring, the effect is comparatively smaller. This is due to the fact that, with the un-tensioned spring, the range of softening springs that guarantee stable equilibrium is smaller. Therefore, the coefficient $k_3 < 0$ for the cubic term was chosen comparatively smaller than that for the pre-tensioned spring. The graph shows a second important feature, since for higher frequencies than the natural frequency, i.e. $\omega > \omega_1$, the spectrum levels at a higher value than that obtained with the linear isolator, that is the specific unbalance $e = m_s r/m$. The dashed line in Plot b of Fig. 8 shows a rather large reduction of the peak response at the fundamental resonance frequency whereas, at higher frequencies, the spectrum is characterised by a constant rise with frequency, which is shifted slightly below than that generated by the linear spring isolator.

## Isolator with Linear Spring and Non-linear Damper

The effects produced by a suspension with a negative quadratic non-linear damper (solid blue line in Fig. 2b) are now examined. In this case, the analysis is based on the lumped parameter model shown in Fig. 9, where the physical properties of the lumped elements are summarised in Table 1.

Here, the restoring force exerted by the damper is given by the following constitutive law:

$$f_c(t) = c_1\dot{x}(t) + c_2\dot{x}(t)|\dot{x}(t)|, \tag{34}$$

where the quadratic damping coefficient is negative, i.e. $c_2 < 0$ [28]. Therefore, using Eqs. (34) and (2) into Eq. (1), the equation of motion results

$$m\ddot{x} + k_l x + c_1\dot{x} + c_2\dot{x}|\dot{x}| = m_s r\omega^2 \sin(\omega t + \theta). \tag{35}$$

Also in this case, the steady-state periodic response of the machine is derived using the harmonic balance method [41–44], which, as discussed in "Appendix A: Harmonic Balance Method" section, assumes the periodic response is approximated by a Fourier series and considers only the fundamental component of the series, such that

$$x(t) = X_1 \sin(\omega t). \tag{36}$$

Accordingly, substituting Eq. (36) into Eq. (35), after some mathematical manipulations and ignoring the higher order harmonic terms in $\sin(3\omega t)$, $\cos(3\omega t)$, gives the following ordinary equation:

$$\left(-m\omega^2 + k_l\right)^2 X_1^2 + \left(c_1 + \frac{3}{\pi}c_2\omega X_1\right)^2 \omega^2 X_1^2 = m_s^2 r^2 \omega^4. \tag{37}$$

The term in round brackets, can be defined as an equivalent damping factor

$$c_{eq}(\omega, X_1) = c_1 + \frac{3}{\pi}c_2\omega X_1. \tag{38}$$

In this case, Eq. (37) can be rewritten in a similar form as Eq. (7), which was derived for the machine mounted on a linear spring and linear damper isolator. Therefore, the spectrum for the vibration amplitudes of the machine mounted on the linear spring and quadratic non-linear damper should replicate that found for the machine mounted on the linear spring-damper isolator. However, according to Eq. (38), for a negative quadratic damping, i.e. for $c_2 < 0$, the damping effect decreases linearly with the frequency and with the amplitude of the response itself. Therefore, the amplitude of the response has to be derived numerically from Eq. (37).

According to Eq. (3), the force transmitted to the base is given by:

$$f_t(t) = k_l x(t) + c_1\dot{x}(t) + c_2\dot{x}(t)|\dot{x}(t)|. \tag{39}$$

Assuming the harmonic vibration given by Eq. (36) and recalling that, for harmonic motion, the displacement and velocity are in quadrature, such that the harmonic forces transmitted by the spring and damper are also 90° out of phase, the amplitude of the time-harmonic total force transmitted to the floor results given by:

$$F_t(\omega) = \sqrt{k_l^2 + \left(c_1 + \frac{3}{\pi}c_2\omega X_1\right)^2}\,\omega^2 X_1. \tag{40}$$

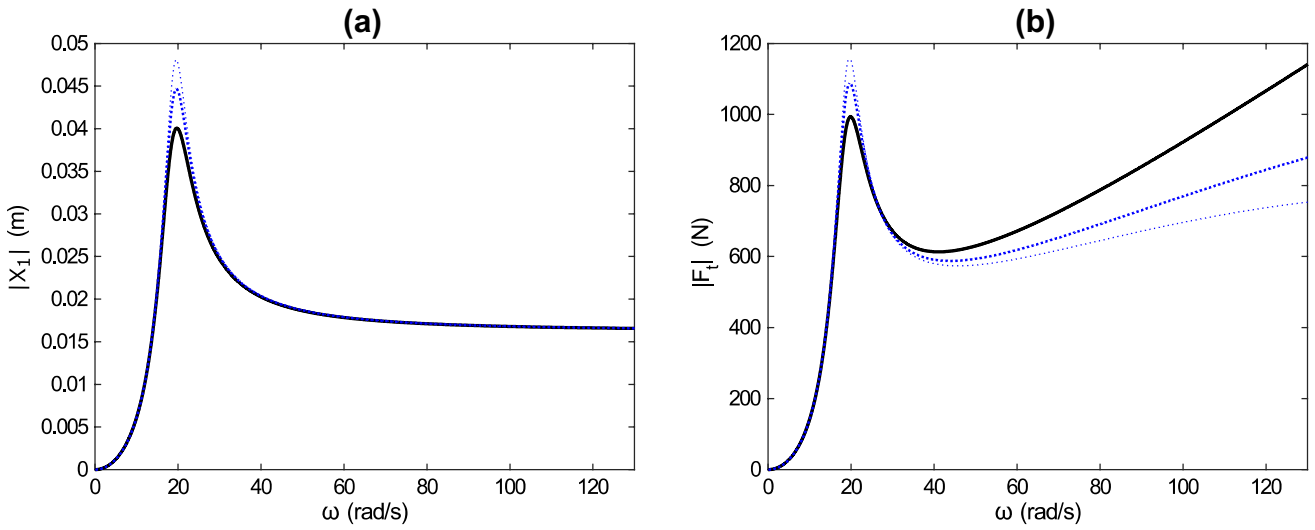


**Fig. 10** Spectra of the vibration (**a**) and force transmission (**b**) amplitudes of the machine mounted on the reference linear spring-damper isolator (thick solid black lines) and on a non-linear isolator with negative quadratic damper (dotted blue lines) (colour figure online)

Similarly to what found for the linear isolator in Eq. (11), this expression suggests that the force transmission to the floor is proportional to the machine vibration amplitude $X_1(\omega)$ and to the machine angular velocity $\omega$ of the rotating unbalance mass, via the damping factor. However, in this case, the damping factor varies with frequency and also with the amplitude of the response itself.

Figure 10 shows the spectra for the vibration (Plots a) and force transmission (Plots b) amplitudes of the machine mounted on the reference spring-damper linear isolator (thick solid black lines) and on the isolator with the non-linear negative quadratic damper (dotted blue lines). To guarantee a fair comparison with the results presented for the machine mounted on the reference linear isolator and the isolator with the non-linear spring, the linear coefficient for the damper has been set such that $c_1 = c_l$ whereas the values reported in Table 1 have been assumed for the negative quadratic coefficient. Considering first Plot a, as discussed above, the spectrum of the machine vibration amplitude is indeed similar to that obtained for the linear isolator in Fig. 4a. In particular, the resonance peak is not tilted and, thus does not show the double branch effect such that the response would be characterised by the jump phenomenon. Therefore, the resonance frequency is not affected by the non-linear damping. Nevertheless, in this case, for increasingly larger values of the negative quadratic damping coefficient $c_2$, the amplitude of the peak response at resonance frequency tends to rise quite significantly. Instead, the response at higher frequencies progressively levels to the specific unbalance $e = m_s r/m$. The spectrum for the amplitude of the force transmitted to the floor shown in plot Plot b, is also quite similar to that depicted in Fig. 4b for the machine mounted on the linear isolator. Therefore, the resonance peak is not tilted and, for increasingly larger values of the negative quadratic damping coefficient $c_2$, the amplitude of the peak force transmission to the floor at resonance frequency rises significantly. Instead, at higher frequencies, the linearly rising force transmission effects is progressively attenuated as the amplitude of the negative quadratic damping effect is brought up. These results seem to indicate that the non-linear quadratic damper could beneficially mitigate the force transmission at higher frequencies above the resonance frequency of the suspended machine. However, this would be accompanied by a significant increment of the machine vibration and force transmission at the fundamental resonance frequency. This would therefore suggest that the negative quadratic non-linear damper is actually not suitable for the purpose of reducing machine vibration and force transmission of an unbalanced rotating machine. However, one may readily notice that it could instead effectively used in combination with a non-linear spring as discussed in "Isolator with Non-linear Spring and Linear Damper" section. Therefore, the following section is dedicated to the analysis of a non-linear suspension encompassing both the non-linear spring and the non-linear damper elements studied in "Isolator with Non-linear Spring and Linear Damper" and "Isolator with Linear Spring and Non-linear Damper" sections.

## Isolator with Non-linear Spring and Non-linear Damper

The effects produced by an isolator with a non-linear spring and non-linear damper are finally examined in this section. Based on the analysis presented in "Isolator with Non-linear

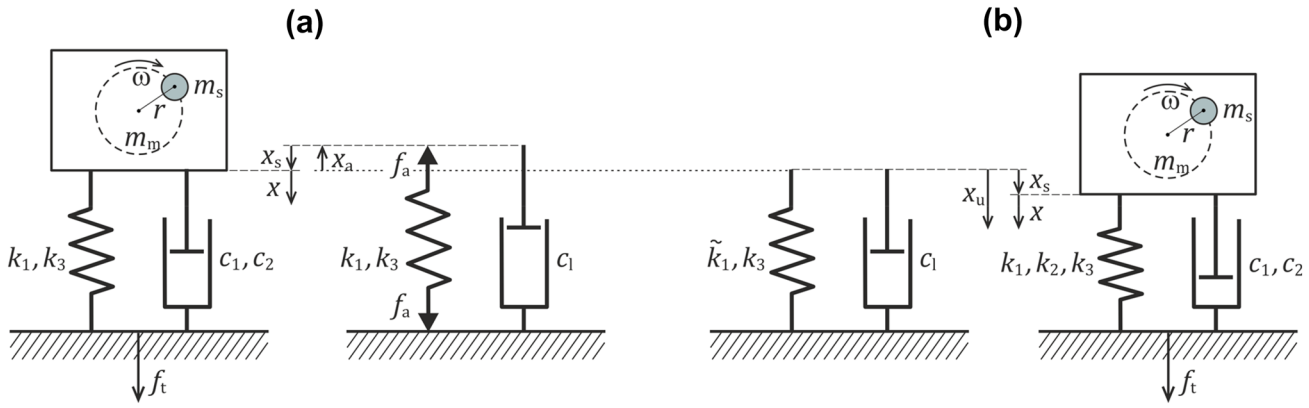


**Fig. 11** Lumped parameter model of the spinning unbalanced machine mounted on pre-tensioned (**a**) and un-tensioned (**b**) cubic non-linear spring and negative quadratic non-linear damper isolator

Spring and Linear Damper" section, a softening cubic non-linear spring is employed to reduce the amplitude of the machine vibration and force transmission to ground at the fundamental resonance frequency of the machine-isolator system. Both, the effects of a pre-tensioned and an un-tensioned spring are investigated. Also, recalling the results presented in "Isolator with Linear Spring and Non-linear Damper" section, a negative quadratic non-linear damper is used to lessen the force transmission to the floor at higher frequencies than the fundamental resonance frequency of the machine-isolator system. Therefore, the analysis is now based on the lumped parameter model shown in Fig. 11, with the physical properties of the lumped elements summarised in Table 1.

## Isolator with a Pre-tensioned Non-linear Spring and a Non-linear Damper

When, as shown in Fig. 11a, the machine is mounted on a pre-tensioned softening cubic spring and a negative quadratic non-linear damper, the equations of motion can be derived by combing the formulations presented in "Isolator with a Pre-tensioned Spring" and "Isolator with Linear Spring and Non-linear Damper" sections for the isolators with the pre-tensioned softening non-linear spring and non-linear damper respectively. Therefore, considering Eqs. (1), (17), (34), the equation of motion can be readily derived in the following form

$$m\ddot{x}(t) + c_1\dot{x}(t) + c_2\dot{x}(t)|\dot{x}(t)| + k_1x(t) + k_3x(t)^3 = m_s r\omega^2 \sin(\omega t + \theta). \tag{41}$$

As discussed in "Isolator with a Pre-tensioned Spring" section, the weight of the machine is balanced by the pre-tensioning effect of the spring such that, when the machine is set into motion and generates the harmonic unbalance force, the cubic non-linear spring produces a symmetric restoring force. Using the harmonic balance method [41–44], which, as discussed in "Appendix A: Harmonic Balance Method" section, considers only the fundamental component of the Fourier series to approximate the periodic response, the steady-state periodic response of the machine is taken equal to

$$x(t) = X_1 \sin(\omega t). \tag{42}$$

Thus, substituting Eq. (42) into Eq. (41), after some mathematical manipulations and neglecting the term in $\sin(3\omega t)$, $\cos(3\omega t)$ the following equation is derived with respect to $X_1(\omega)$:

$$\left(-m\omega^2 + k_1 + \frac{3}{4}k_3X_1^2\right)^2 X_1^2 + \left(c_1 + \frac{3}{\pi}c_2\omega X_1\right)^2 \omega^2 X_1^2 = m_s^2 r^2 \omega^4. \tag{43}$$

As done in "Isolator with a Pre-tensioned Spring" section, this equation is solved numerically by finding the values of $\omega$ with reference to a range of amplitudes $X_1$ that guarantee real positive solutions, i.e. $\omega > 0$. In this case too, the resulting function $X_1(\omega)$ is not uniquely defined at frequencies close to the resonance frequency. Indeed, as found in "Isolator with a Pre-tensioned Spring" section for the softening-spring, three values of $X_1(\omega)$ may satisfy Eq. (41) at frequencies slightly lower than the resonance frequency, which leads to the typical two branches spectrum of $X_1(\omega)$, that is the left hand side tilted resonance peak.

According to Eq. (9), the amplitude of the force transmitted to ground is in this case given by:

$$f_t = k_1x + k_3x^3 + c_1\dot{x} + c_2\dot{x}|\dot{x}|. \tag{44}$$

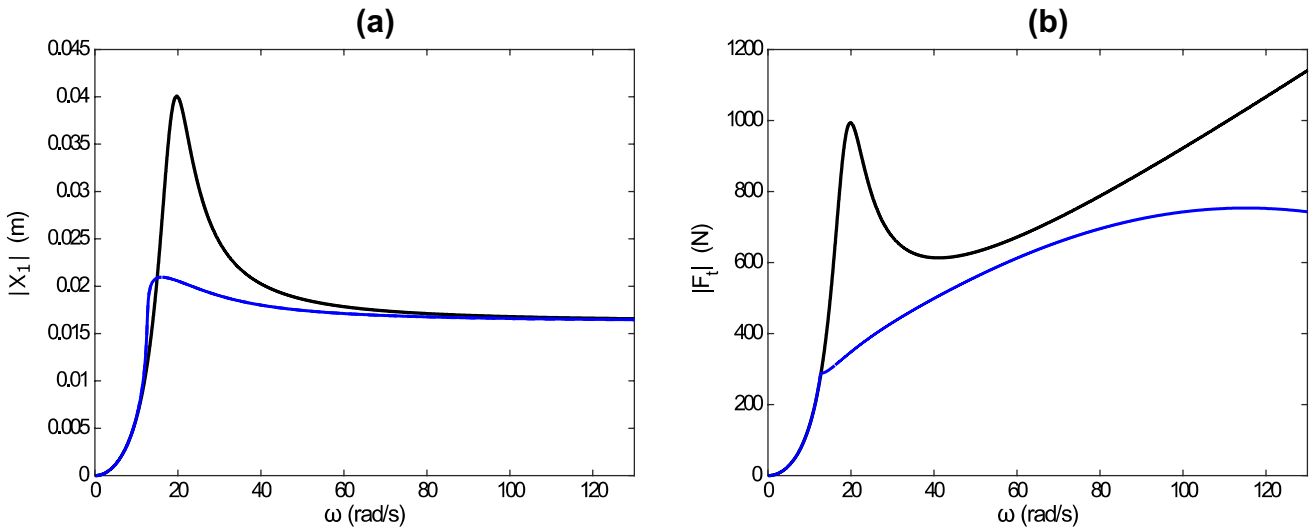


**Fig. 12** Spectra of the vibration (**a**) and force transmission (**b**) amplitudes of the machine mounted on the reference linear spring-damper isolator (thick solid black lines) and on a pre-tensioned non-linear isolator with softening cubic spring and negative quadratic damper (thick solid blue lines) (colour figure online)

Therefore, using Eqs. (42), (43), and recalling that for harmonic motion the elastic and damping forces are 90° out of phase, the amplitude of the force transmitted to the floor by the spring and damper results given by:

$$F_t = \sqrt{\left(k_1 X_1 + \frac{3}{4}k_3 X_1^3\right)^2 + \left(c_1 + \frac{3}{\pi}c_2 \omega X_1\right)^2 \omega^2 X_1^2}. \quad (45)$$

As done in the previous sections, to guarantee a fair comparison with the results presented for the machine mounted on the reference linear isolator, the linear coefficients for the spring have been set such that $k_1 = k_l$. Also, the concurrent non-linear effects of the pre-tensioned softening cubic spring, the linear positive damper and negative quadratic damper have been optimised with a parametric study. Three conditions were considered with reference to the vibration and force transmission to the floor when the machine is mounted on the linear isolator. First, at least a 50% reduction of the machine vibration peak amplitude at resonance frequency. Second, at least a 30% reduction of the force transmission amplitude at the maximum spinning velocity of 120rad/s. Third, prevention of the jump phenomenon, which is undesirable in practical situations. Table 1 reports the non-linear stiffness and damping coefficients found from the parametric study and thus employed to generate the simulation results presented in this section.

Figure 12 shows the spectra for the vibration (Plots a) and force transmission (Plots b) amplitudes of the machine mounted on the reference spring-damper linear isolator (thick solid black lines) and on isolator with the pre-tensioned softening non-linear spring and the non-linear damper (thin solid blue lines). The two plots clearly indicate that the combined effects of the pre-tensioned softening non-linear spring and non-linear damper effectively reduce both the peak machine vibration and force transmission at the fundamental resonance frequency and the force transmission at the higher spinning velocity of the machine. Moreover, the fundamental resonance frequency is shifted to significantly lower values. At higher frequencies than the fundamental resonance frequency, the amplitude of the machine vibration still converges to the relative unbalance. As discussed in "Isolator with Linear Spring and Linear Damper" section, above resonance frequency, the amplitude of the machine vibration solely depends on the machine and unbalance properties. Therefore, regardless the linear or non-linear isolators are employed, the amplitude of the machine vibration is bound to oscillate with amplitude $e = m_s r/m$.

Although the optimisation of the non-linear stiffness and non-linear damping parameters was based on the amplitude of the machine response at the fundamental resonance frequency, Plot b of Fig. 12 shows quite a significant reduction of the transmitted force to the floor at resonance frequency. This is due to the fact that the softening spring produces two concurrent effects at low frequencies. On one hand, it tilts on the left hand side the resonance peak so that the resonance frequency is lowered and, rather importantly, the amplitude of the peak response is reduced too. On the other hand, since at low frequencies the force transmission to the floor primarily occurs via the softened spring, it also reduces the force transmissibility.

### Isolator with an Un-tensioned Non-Linear Spring and a Non-Linear Damper

In the second case, where, as shown in Fig. 11b, the machine is mounted on an un-tensioned softening cubic spring and a negative quadratic non-linear damper, the equations of motion are derived by combing the formulations presented in "Isolator with an Un-tensioned Spring" section, for the isolators with the un-tensioned softening non-linear spring, and in "Isolator with Linear Spring and Non-linear Damper" section, for the isolator with the non-linear damper. Therefore, considering Eqs. (1), (25), (34), the equation of motion can be readily derived in the following form

$$m\ddot{x}(t) + c_1\dot{x}(t) + c_2\dot{x}(t)|\dot{x}(t)| + k_1x(t) + k_2x(t)^2 + k_3x(t)^3 = m_s r\omega^2 \sin(\omega t + \theta), \tag{46}$$

where $k_1$ and $k_2$ are given by Eqs. (27) and (28), that is $k_1 = \widetilde{k}_1 + 3k_3{x_{st}}^2$ and $k_2 = 3k_3x_{st}$. As discussed in "Isolator with an Un-tensioned Spring" section, in this case, the weight of the machine generates a static compression of the spring such that the cubic non-linear stiffness of the spring produces an asymmetric restoring force. Employing the harmonic balance method discussed in "Appendix A: Harmonic Balance Method" section [41–44], such that the machine displacement is approximated with the fundamental component of the Fourier series of the periodic response, that is

$$x(t) = X_0 + X_1 \sin(\omega t), \tag{47}$$

the following two equations are derived with respect to $X_0$ and $X_1$ from Eq. (46):

$$\left((-m\omega^2 + k_1 + 2k_2X_0 + 3k_3X_0^2)X_1 + \frac{3}{4}k_3X_0^3\right)^2 + \left(c_1 + \frac{3}{\pi}c_2\omega X_1\right)^2\omega^2X_1^2 = m_s^2r^2\omega^4, \tag{48}$$

$$k_3X_0^3 + k_2X_0^2 + \left(k_1 + \frac{3}{2}k_3X_1^2\right)X_0 + \frac{1}{2}k_2X_1^2 = 0. \tag{49}$$

The solution of Eq. (49) was derived analytically in closed form assuming $X_0$ and solving for $X_1$. Equation (48) is a fourth order equation in frequency, which has been solved numerically by finding the values of $\omega$ for a range of amplitudes $X_1$ that guarantee real positive solutions, i.e. $\omega > 0$.

In this case, neglecting the weight of the machine, recalling Eq. 9 the force transmitted to ground is given by:

$$f_t(t) = k_1x(t) + k_2x(t)^2 + k_3x(t)^3 + c_1\dot{x}(t) + c_2\dot{x}(t)|\dot{x}(t)|. \tag{50}$$

Therefore, using the expression for $x(t)$ given in Eq. (47) and the values of $X_0$ and $X_1$ derived from Eqs. (48), (49), and recalling that, for harmonic motion, the elastic and damping forces are 90° out of phase, the force transmitted the floor by the spring and damper was derived in terms of the following expression:

$$F_t = \left(k_1X_0 + k_2X_0^2 + k_3X_0^3 + \frac{1}{2}(3k_3X_0 + k_2)X_1^2\right) + X_0^2\sqrt{\left(k_1X_0 + \frac{3}{4}k_3X_1^3 + 3k_3X_0^2X_1 + 2k_2X_0X_1\right)^2 + \left(c_1\omega X_1 + \frac{3}{\pi}c_2\omega^2X_1^2\right)^2}. \tag{51}$$

Figure 13 shows the spectra for the vibration (Plots a) and force transmission (Plots b) amplitudes of the machine mounted on the reference spring-damper linear isolator (thick black solid lines) and on isolator with the un-tensioned softening non-linear spring and the non-linear damper (thick blue solid lines). Also in this case, to ensure the results can be compared with those obtained for the machine mounted on the reference linear isolator, the linear $\widetilde{k}_1$ and non-linear $k_3$ coefficients for the spring have been set such that $k_1 \cong k_l$. Moreover, the linear and non-linear damping coefficients have been selected in such a way as, with reference to the vibration and force transmission to the floor when the machine is mounted on the linear isolator, there is at least a 30% reduction of the machine vibration peak amplitude, without the instability effect that generates the jump phenomenon, and a 30% reduction of the force transmission amplitude at the maximum spinning velocity of 120rad/s.

The two plots in Fig. 13 show similar results than those found for the isolator with the pre-tensioned spring. Indeed, the un-tensioned non-linear softening spring and the non-linear damper effectively control the peak machine vibration and the force transmission at the fundamental resonance frequency, which is shifted to significantly lower values. Also, they successfully control the force transmission at the higher spinning velocity of the machine. However, as noticed in "Isolator with an Un-tensioned Spring" section, the un-tensioned spring generates at higher frequencies than the fundamental resonance frequency a comparatively larger machine vibration amplitude than

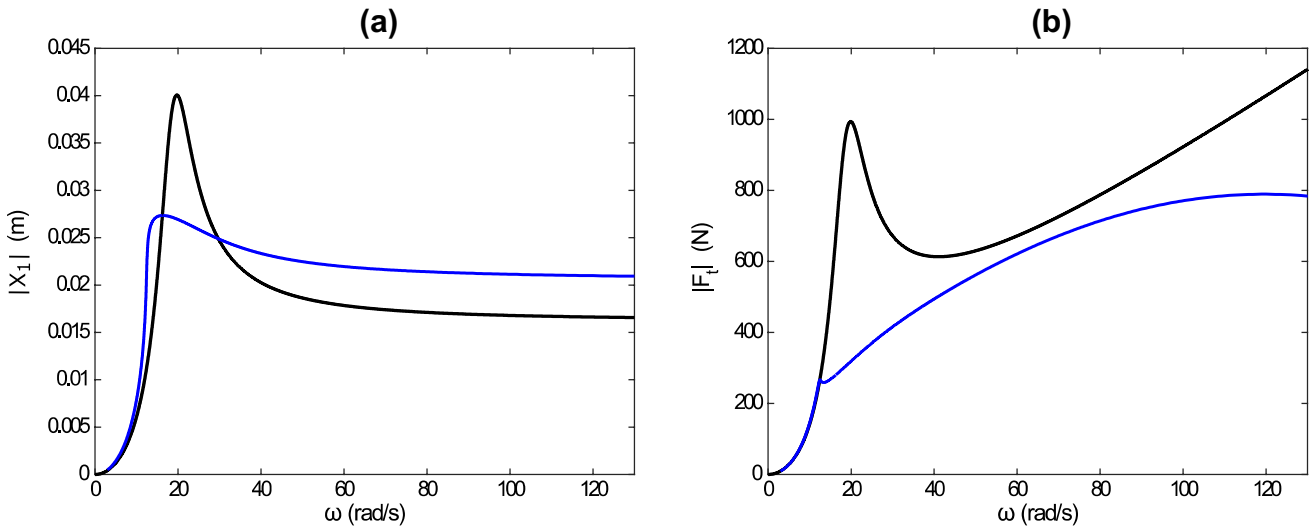


**Fig. 13** Spectra of the vibration (**a**) and force transmission (**b**) amplitudes of the machine mounted on the reference linear spring-damper isolator (thick solid black lines) and on an un-tensioned non-linear isolator with softening cubic spring and negative quadratic damper (thick solid blue lines) (colour figure online)

the relative unbalance $e = m_s r/m$. Moreover, the peak vibration response at the resonance frequency is slightly higher than that produced by the isolator equipped with pre-tensioned spring. As for the configuration with the pre-tensioned spring, Plot b of Fig. 13 shows a rather large reduction of the transmitted force to the floor at resonance frequency. Again, this is due to two concurrent effects of the softening spring, which on one hand tilts on the left hand side and reduces the amplitude of the resonance peak, and, on the other hand, reduces the low frequency force transmission to the floor, which, indeed, primarily occurs via the softened spring.

## Conclusions

This paper has presented a theoretical study on the vibration and force transmission control of an unbalanced rotating machine mounted on different arrangements of isolators formed by linear or non-linear cubic softening/hardening un-tensioned/pre-tensioned springs connected in parallel with linear or non-linear quadratic dampers. A concise and consistent formulation based on the harmonic balance approach has been derived for all combinations of the linear and non-linear spring and damper elements. To guarantee a representative study, an accurate analysis of the equilibrium points has been carried out and summarised in the Appendix to ensure the response of the machine mounted on the proposed non-linear isolators is stable.

The study has shown that, the best vibration isolation is provided by a pre-tensioned linear and cubic softening spring combined with a linear and negative quadratic damper. The pre-tensioned spring should be designed in such a way as it holds the weight of the machine and thus produces on the vibrating machine a symmetric elastic restoring force proportional to the linear and cubic powers of the displacement. The cubic softening stiffness should then be tuned to minimise the frequency, and thus the amplitude, of the resonant response of the fundamental mode of the machine and elastic suspension system, while preserving stability and a desired static deflection. In parallel, to reduce the force transmission to ground above the fundamental resonance frequency, the negative quadratic damping effect should be tailored to maximise the energy absorption at higher frequencies.

The study has also highlighted that, isolators with hardening springs shift to higher values the fundamental resonance frequency such that the peak response of the suspended machine is increased rather than attenuated. Moreover, when un-tensioned non-linear springs are used, at higher frequencies than the fundamental resonance, the machine vibration is higher than the specific unbalance. Lastly, the study has shown that, at low frequencies close to the fundamental resonance frequency of the suspended machine, the negative quadratic damping tends to reduce the linear damping effect. Therefore, it should be carefully tuned in such a way as to produce the desired reduction of machine vibration and force transmission at higher frequencies without compromising the vibration and force transmission control at the fundamental resonance frequency.

## Appendix A: Harmonic Balance Method

This appendix provides the solutions of the non-linear equations of motion for the machine mounted on the non-linear isolators, which have been derived using the harmonic balance method [41–44]. The equations of motion for the more general configurations of "Isolator with Non-linear Spring and Non-linear Damper" section are considered, where the isolator is composed by the pre-tensioned and un-tensioned cubic non-linear spring and by the negative quadratic damper.

### Machine Mounted on the Non-linear Pre-tensioned Spring

According to "Non-linear Isolator with a Pre-tensioned Non-linear Spring and a Non-linear Damper" section, when the unbalanced machine is mounted on the pre-tensioned spring, the dynamic response of the machine is governed by Eq. (41), that is

$$m\ddot{x}(t) + c_1\dot{x}(t) + c_2\dot{x}(t)|\dot{x}(t)| + k_1x(t) + k_3x(t)^3 = m_sr\omega^2\sin(\omega t + \theta). \tag{52}$$

The harmonic balance method [41–44] assumes the periodic response is approximated by a Fourier series and considers only the fundamental component of the series, such that

$$x(t) = X_1\sin(\omega t). \tag{53}$$

Substituting Eq. (53) into Eq. (52) yields:

$$\begin{aligned}&\left(-m\omega^2 + k_1\right)X_1\sin(\omega t) + c_1\omega X_1\cos(\omega t)\\ &+c_2\omega^2X_1^2\cos(\omega t)^2 sign\left(\omega X_1\cos(\omega t)\right)\\ &+k_3X_1^3\sin(\omega t)^3 = m_sr\omega^2\sin(\omega t + \theta),\end{aligned} \tag{54}$$

As discussed in Ref. [27], the Fourier series for sign($\omega X\cos(\omega t)$) in Eq. (54) is the same as that for a square wave, having the fundamental component of $\frac{4}{\pi}cos(\omega t)$. Thus, substituting the fundamental component of the Fourier series for the square wave into Eq. (54), expanding the harmonic terms and neglecting the higher order harmonics gives:

$$\begin{aligned}&\left(\left(k_1 - m\omega^2\right)X_1 + \frac{3}{4}k_3X_1^3\right)\sin(\omega t)\\ &+\left(c_1 + \frac{3}{\pi}c_2\right)\omega X_1\cos(\omega t)\\ &= m_sr\omega^2(\sin(\omega t)\cos(\theta) + \sin(\theta)\cos(\omega t)).\end{aligned} \tag{55}$$

Equating the sine and cosine terms in Eq. (55) and adding the squares of these two terms, yields

$$\begin{aligned}&\left(-m\omega^2 + k_1 + \frac{3}{4}k_3X_1^2\right)^2X_1^2\\ &+\left(c_1 + \frac{3}{\pi}c_2\omega X_1\right)^2\omega^2X_1^2 = m_s^2r^2\omega^4.\end{aligned} \tag{56}$$

Contrary to the approach normally used for linear systems, this equation is solved numerically for the values of $\omega$ with reference to a range of amplitudes $X_1$ that guarantee real positive solutions, i.e. $\omega > 0$. Nevertheless, the peak amplitude of the response at resonance frequency can be derived analytically. Indeed, differentiating both sides of Eq. (56) with respect to $\omega$ gives:

$$\frac{dX_1}{d\omega} = \frac{4m\omega X_1^2\left(-m\omega^2 + k_1 + \frac{3}{4}k_3X_1^2\right) - 2\omega X_1^2c_1^2 + 4m_s^2r^2\omega^3}{2X_1\left(-m\omega^2 + k_1 + \frac{3}{4}k_3X_1^2\right)^2 + 2X_1c_1^2\omega^2 + 3k_3X_1^3\left(-m\omega^2 + k_1 + \frac{3}{4}k_3X_1^2\right)}. \tag{57}$$

The maximum amplitude occurs when $\frac{dX_1}{d\omega} = 0$, that is when the numerator of Eq. (57) is equal to 0 (for non-zero denominator), that is:

$$4m\omega X_1^2\left(-m\omega^2 + k_1 + \frac{3}{4}k_3X_1^2\right) - 2\omega X_1^2c_1^2 + 4m_s^2r^2\omega^3 = 0. \tag{58}$$

Solving for $\omega^2$ yields:

$$\omega^2 = \frac{X_1^2\left(\frac{3}{4}mk_3X_1^2 + mk_1 - \frac{c_1^2}{2}\right)}{m^2X_1^2 - m_s^2r^2}. \tag{59}$$

Assuming $\omega_1 = \sqrt{k_1/m}, \xi_1 = c_1/2\omega_1m$, $e = m_sr/m$ and $\beta_3 = k_3/m$, Eq. (59) can be rewritten as follows:

$$\omega^2 = \frac{\left(\frac{3}{4}\beta_3X_1^2 + \omega_1^2 - 2\xi_1^2\omega_1^2\right)}{1 - \frac{e^2}{X_1^2}}. \tag{60}$$

Now, assuming that relative eccentricity is small compared to the peak response i.e. $e \ll X_{mx}$, for small damping ratio i.e. $\xi_1 \ll 0.5$, the frequency for the peak response results given by:

$$\omega_{mx}^2 = \frac{\left(\frac{3}{4}k_3X_1^2 + k_1\right)}{m} = \frac{3}{4}\beta_3X_1^2 + \omega_1^2. \tag{61}$$

Substituting this result into Eq. (56) yields:

$$\mathrm{X}_{1,mx} = \sqrt{\frac{k_1}{m\frac{c_1^2}{m_s^2r^2} - \frac{3}{4}k_3}} = \frac{\omega_1}{\sqrt{\left(\frac{2\xi_1\omega_1}{e}\right)^2 - \frac{3}{4}\beta_3}}. \tag{62}$$

Going back to "Non-linear Isolator with a Pre-tensioned Non-linear Spring and a Non-linear Damper" section, the force transmitted to the floor is given by Eq. (44), that is

$$f_t = k_1 x + k_3 x^3 + c_1 \dot{x} + \mathrm{c}_2 \dot{x}|\dot{x}|. \tag{63}$$

Therefore, substituting the approximate solution given in Eq. (53), the force transmitted to the floor results given by:

$$\begin{aligned} f_t = {} & k_1 X_1 \sin(\omega t) + k_3 X_1^3 \sin(\omega t)^3 \\ & + c_1 \omega X_1 \cos(\omega t) \\ & + \mathrm{c}_2 \omega^2 X_1^2 \cos(\omega t)^2 \mathrm{sign}\big(\omega X_1 \cos(\omega t)\big), \end{aligned} \tag{64}$$

which, using trigonometric identities, neglecting the higher order harmonic terms and assuming $\mathrm{sign}\big(\omega X_1 \cos(\omega t)\big) = \frac{4}{\pi} cos(\omega t)$, yields:

$$\begin{aligned} f_t = {} & \left(k_1 X_1 + \frac{3}{4} k_3 X_1^3\right) \sin(\omega t) \\ & + \left(c_1 + \frac{3}{\pi} \mathrm{c}_2 \omega X_1\right) \omega X_1 \cos(\omega t), \end{aligned} \tag{65}$$

Since the terms in $\sin(\omega t)$ and $\cos(\omega t)$ are in quadrature, the amplitude of the transmitted force results given by:

$$F_t = \sqrt{\left(k_1 X_1 + \frac{3}{4} k_3 X_1^3\right)^2 + \left(c_1 + \frac{3}{\pi} \mathrm{c}_2 \omega X_1\right)^2 \omega^2 X_1^2}. \tag{66}$$

## Machine Mounted on the Non-linear Un-tensioned Spring

Moving to "Non-linear Isolator with an Un-tensioned Spring" section, when the unbalanced machine is mounted on the un-tensioned spring, the dynamic response of the machine is governed by Eq. (46), that is

$$\begin{aligned} & m\ddot{x}(t) + c_1 \dot{x}(t) + \mathrm{c}_2 \dot{x}(t)|\dot{x}(t)| + k_1 x(t) + k_2 x(t)^2 + k_3 x(t)^3 \\ & = m_s r \omega^2 \sin(\omega t + \theta), \end{aligned} \tag{67}$$

Also in this case, according to the harmonic balance method [41–44], the periodic response is assumed equal to the fundamental component of the Fourier series that approximates the periodic response, such that

$$x(t) = X_0 + X_1 \sin(\omega t), \tag{68}$$

where, as discussed in [40], $X_1$ is the amplitude of the steady-state harmonic machine vibration and $X_0$ is the displacement offset with respect to the static displacement generated when the machine is mounted on the isolator. This offset is generated by the non-symmetric restoring elastic force caused by un-tensioned non-linear cubic spring, which, as can be readily deduced from Eq. (67), leads to both quadratic and cubic restoring force terms. Substituting Eq. (68) into Eq. (67) yields:

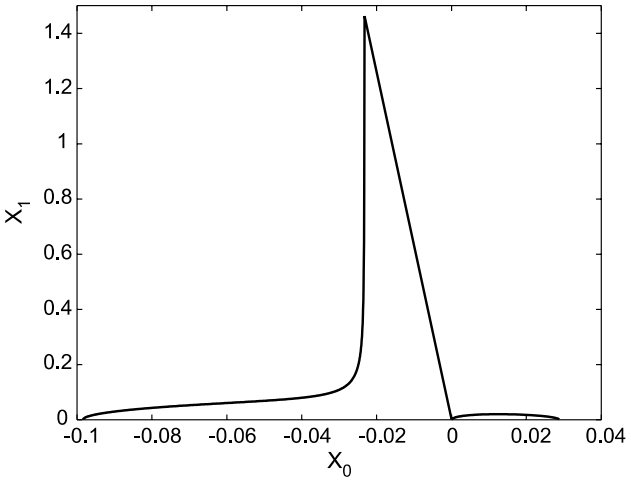


**Fig. 14** Example of numerical solutions obtained from Eq. (74)

$$\begin{aligned} & \left(\left(-m\omega^2 + k_1\right) X_1 + \frac{3}{4} k_3 X_1^3 + \left(2k_2 X_0 + 3k_3 X_0^2\right) X_1\right) \sin(\omega t) \\ & + \left(c_1 \omega X_1 + \frac{3}{\pi} c_2 \omega^2 X_1^2\right) \cos(\omega t) + k_3 X_0^3 + k_2 X_0^2 \\ & + \left(k_1 + \frac{3}{2} k_3 X_1^2\right) X_0 + \frac{1}{2} k_2 X_1^2 \\ & = m_s r \omega^2 [\sin(\omega t) \cos(\theta) + \cos(\omega t) \sin(\theta)], \end{aligned} \tag{69}$$

where the higher order harmonic terms have been neglected. Equating the harmonic components and setting to zero the coefficients of the terms in $X_0$, Eq. (69) result into the following three equations:

$$\begin{aligned} & \left(-m\omega^2 + k_1\right) X_1 + \frac{3}{4} k_3 X_1^3 + \left(2k_2 X_0 + 3k_3 X_0^2\right) X_1 \\ & = m_s r \omega^2 \cos(\theta), \end{aligned} \tag{70}$$

$$c_1 \omega X_1 + \frac{3}{\pi} c_2 \omega^2 X_1^2 = m_s r \omega^2 \sin(\theta), \tag{71}$$

$$k_3 X_0^3 + k_2 X_0^2 + \left(k_1 + \frac{3}{2} k_3 X_1^2\right) X_0 + \frac{1}{2} k_2 X_1^2 = 0. \tag{72}$$

Finally, squaring and adding Eqs. (70) and (71), the three equations above can be casted in the following two equations:

$$\begin{aligned} & \left(\left(-m\omega^2 + k_1\right) X_1 + \frac{3}{4} k_3 X_1^3 + \left(2k_2 X_0 + 3k_3 X_0^2\right) X_1\right)^2 \\ & + \left(c_1 \omega X_1 + \frac{3}{\pi} c_2 \omega^2 X_1^2\right)^2 = m_s r \omega^2, \end{aligned} \tag{73}$$

$$k_3 X_0^3 + k_2 X_0^2 + \left(k_1 + \frac{3}{2} k_3 X_1^2\right) X_0 + \frac{1}{2} k_2 X_1^2 = 0. \tag{74}$$

Equation (74) can be solved analytically for $X_1$ assuming $X_0$. Then, the fourth order Eq. (73) can be solved numerically for $\omega$ considering a range of amplitudes $X_1$ that guarantee real positive solutions, i.e. $\omega > 0$. Figure 14 shows the solutions of Eq. (74) for fixed values of $k_1$, $k_2$, $k_3$, derived for different static displacements $X_0$. Eq. (73) has been solved from values of $X_1$ corresponding to positive static displacements $X_0$ only.

According to "Non-linear Isolator with an Un-tensioned Spring" section, the force transmitted to the floor by the un-tensioned non-linear isolator is given by Eq. (50), that is

$$f_t(t) = k_1 x(t) + k_2 x(t)^2 + k_3 x(t)^3 + c_1 \dot{x}(t) + c_2 \dot{x}(t) |\dot{x}(t)|, \tag{75}$$

which, using trigonometric identities and neglecting the higher order harmonic terms yields:

$$f_t = \left(k_1 X_1 + \frac{3}{4} k_3 X_1^3 + \left(2k_2 X_0 + 3k_3 X_0^2\right) X_1\right) \sin(\omega t) + \left(c_1 \omega X_1 + \frac{3}{\pi} c_2 \omega^2 X_1^2\right) \cos(\omega t) + k_3 X_0^3 + k_2 X_0^2 + \left(k_1 + \frac{3}{2} k_3 X_1^2\right) X_0 + \frac{1}{2} k_2 X_1^2. \tag{76}$$

Since the terms in $\sin(\omega t)$ and $\cos(\omega t)$ are in quadrature, the amplitude of the transmitted force results given by:

$$F_t = \sqrt{\left(k_1 X_1 + \frac{3}{4} k_3 X_1^3 + \left(2k_2 X_0 + 3k_3 X_0^2\right) X_1\right)^2 + \left(c_1 \omega X_1 + \frac{3}{\pi} c_2 \omega^2 X_1^2\right)^2} + k_3 X_0^3 + k_2 X_0^2 + \left(k_1 + \frac{3}{2} k_3 X_1^2\right) X_0 + \frac{1}{2} k_2 X_1^2. \tag{77}$$

## Appendix B: Equilibrium Points and Stability Analysis

The stability of the proposed machine—non-linear isolator systems depends on the so-called stability points, that is, those points in the phase plot for the free response of the system where the velocity coordinate goes to zero. The equilibrium points and stability conditions for the machine mounted on the pre-tensioned and un-tensioned springs are therefore examined below with reference to the Jacobian of the system equation of motion given in state space form [47]. More specifically, the focus is on the isolators with softening spring elements, which may lead to instability conditions [48].

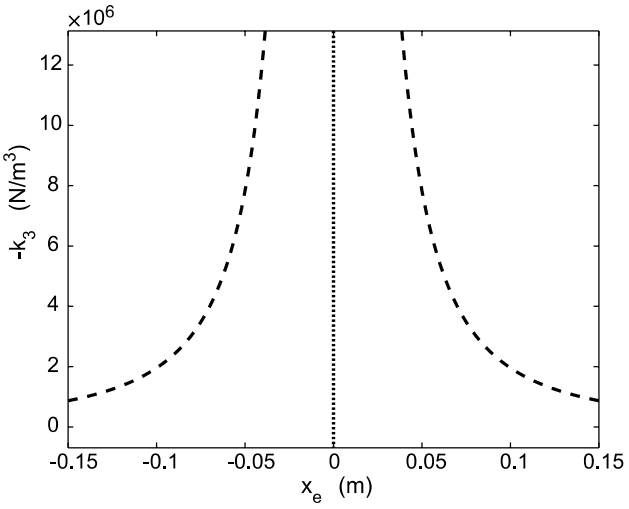


**Fig. 15** Positions of the equilibrium points for different values of the non-linear stiffness parameter $k_3$ of the non-linear softening spring in the pre-tensioned isolator

### Machine Mounted on the Non-linear Pre-tensioned Spring

Recalling the equation of motion, i.e. Eq. (41), for the unbalanced machine mounted on the pre-tensioned spring, the equilibrium points are calculated assuming there is no excitation produced by the rotating mass and setting the acceleration and velocity are equal to zero i.e. $\ddot{x}(t) = \dot{x}(t) = 0$. The equation of motion is thus rewritten in a state-space form:

$$\dot{\mathbf{x}} = f(\mathbf{x}), \tag{78}$$

where $\mathbf{x} = \begin{bmatrix} x_1 \\ x_2 \end{bmatrix} = \begin{bmatrix} x \\ \dot{x} \end{bmatrix}$ is the state vector. Setting, $\ddot{x}(t) = \dot{x}(t) = 0$ three equilibrium points are obtained: the first at $x_{e1} = 0$ and the second and third at $x_{e2,3} = \pm\sqrt{-k_1/k_3}$. Such points identify the local minima and maxima of the potential energy of the system, that is, the static displacement that corresponds to zero net restoring force exerted by the non-linear suspension. The stability of the equilibrium points can be obtained by studying the eigenvalues of the Jacobian associated to the state-space Eq. (78), which is given by:

$$J_c(\mathbf{x}) = \begin{bmatrix} 0 & 1 \\ \left(-\frac{k_1}{m} - 3\frac{k_3}{m} x_1^2\right) & \left(-2\frac{c_2}{m} x_2 sign(x_2) - \frac{c_1}{m}\right) \end{bmatrix}. \tag{79}$$

Considering the first equilibrium point, substituting $x_{e1} = 0$ into Eq. (79), the eigenvalues of the Jacobian matrix result equal to:

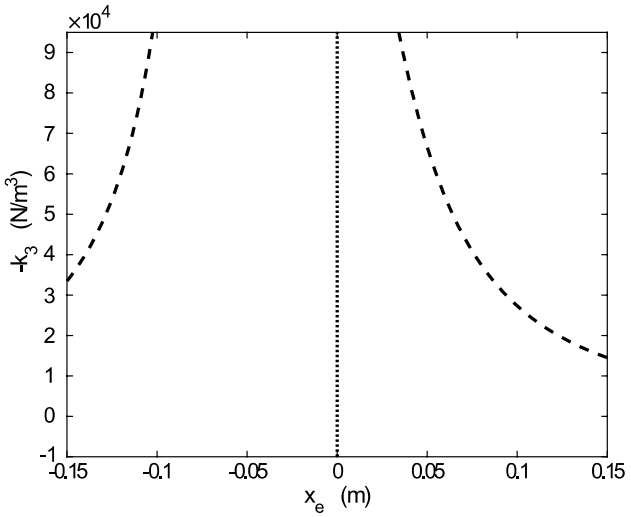


**Fig. 16** Positions of the equilibrium points for different values of the non-linear stiffness parameter $k_3$ of the non-linear softening spring in the un-tensioned isolator

$$\lambda_{e1} = \frac{-c_1 \pm \sqrt{c_1^2 - 4mk_1}}{2m} = -\omega_1\left(\xi_1 \pm \mathrm{j}\sqrt{1-\xi_1^2}\right), \quad (80)$$

where $\omega_1 = \sqrt{k_1/m}$ and $\xi_1 = c_1/(2\omega_1 m)$. Moving to the other two equilibrium points, substituting $x_{e2,3} = \pm\sqrt{-k_1/k_3}$ it into Eq. (79), the eigenvalues of the Jacobian matrix result equal to:

$$\lambda_{e23} = \frac{-c_1 \pm \sqrt{c_1^2 + 4mk_1}}{2m} = -\omega_1\left(\xi_1 \pm \sqrt{2+\xi_1^2}\right), \quad (81)$$

which are real numbers with opposite sign. In this case the equilibrium points are called saddle and the stability of the system in the vicinity of $x_{e2}$, $x_{e3}$, depends on the initial conditions. Figure 15 shows the positions of the equilibrium points for different values of the non-linear stiffness parameter $k_3$. The dotted line represents the stable point $x_{e1}$ whereas the two dashed lines show the positions of the saddle points $x_{e2}$,$x_{e3}$. It is clear that for a fixed linear stiffness $k_1$, increasing the value of the negative stiffness $k_3$ reduces the region of attraction of the stable point $x_{e1}$.

### Machine Mounted on the Non-linear Pre-tensioned Spring

Considering now the equation of motion (46) for the unbalanced machine mounted on the un-tensioned spring, following the procedure described in Appendix "Machine Mounted on the Non-linear Pre-tensioned Spring" section, the study of the equilibrium points gives three solutions, which are given by:

$$x_{e1} = 0, \quad (82)$$

$$x_{e2,3} = \frac{-k_2 \pm \sqrt{k_2^2 - 4k_3k_1}}{2k_3}, \quad (83)$$

where in this case $k_1 = \widetilde{k}_1 + 3k_3{x_{st}}^2$, $k_2 = 3k_3x_{st}$ with $x_{st}$ the static equilibrium point of the system.

Eq. (83) gives two asymmetric points, which correspond to the local maxima of the potential energy of the system around its static equilibrium point. For this system, the Jacobian of the state-space equation of motion (78) is given by

$$\mathbf{J}_u(\mathbf{x}) = \begin{bmatrix} 0 & 1 \\ \left(-\frac{k_1}{m} - 2\frac{k_2}{m}x_1 - 3\frac{k_3}{m}x_1^2\right) & \left(-2\frac{c_2}{m}x_2 sign(x_2) - \frac{c_1}{m}\right) \end{bmatrix}. \quad (84)$$

Therefore, substituting the equilibrium points $x_{e1}$, $x_{e2}$, $x_{e3}$ in it, the eigenvalues result

$$\lambda_{e1} = -\omega_1\left(\xi_1 \pm \mathrm{j}\sqrt{1-\xi_1^2}\right), \quad (85)$$

$$\lambda_{e2} = -\frac{c_1 \pm \sqrt{\frac{c_1^2k_3 - 2k_2^2m + 8mk_1k_3 + 2k_2m\sqrt{k_2^2 - 4k_1k_3}}{k_3}}}{2m}, \quad (86)$$

$$\lambda_{e3} = -\frac{c_1 \pm \sqrt{\frac{c_1^2k_3 - 2k_2^2m + 8mk_1k_3 - 2k_2m\sqrt{k_2^2 - 4k_1k_3}}{k_3}}}{2m}. \quad (87)$$

Similarly to the previous case, the first eigenvalue $\lambda_{e1}$ is complex with negative real part while the second and the third eigenvalues are given by real numbers with opposite sign. It follows that $x_{e1}$ is the only stable equilibrium point. Similarly to Fig. 15, Fig. 16 shows the position of the equilibrium points with respect to the non-linear stiffness $k_3$.

## Appendix C: Forced Response to Harmonic Excitation: Steady-State Stability Analysis

As discussed in "Isolator with Non-linear Spring and Linear Damper", "Isolator with Linear Spring and Non-linear Damper" and "Isolator with Non-linear Spring and Non-linear Damper" sections, the response of the unbalanced spinning machine mounted on isolators with non-linear spring elements is characterised by frequency regions in the vicinity of resonance frequency where the amplitude of the response is not uniquely defined and thus the so-called "jump phenomenon"

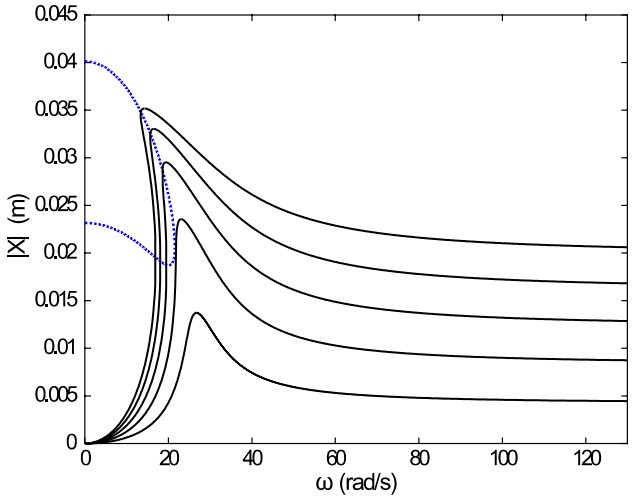


**Fig. 17** Spectra of the vibration amplitudes (thick solid black lines) and unstable region (thin solid blue line) of the machine mounted on the non-linear isolator with softening cubic spring and negative quadratic damper with reference to increasingly larger unbalanced masses (colour figure online)

takes place [41–45]. This phenomenon can be regarded "in some sense" as an instability effect, which is thus investigated in this appendix for the machine mounted on the pre-tensioned isolator with cubic non-linear spring. Following the formulation proposed in Ref. [42], the steady-state solution $x_{ss}(t)$ of the equation of motion, i.e. Equation (41), is considered with, superimposed, a small perturbation $e$:

$$x(t) = x_{\mathrm{ss}}(t) + e. \tag{88}$$

Thus substituting Eq. (88) into Eq. (41), yields:

$$m\left(\ddot{x}_{\mathrm{ss}} + \ddot{e}\right) + \left(c_1 + \mathrm{c}_2\left|\dot{x}_{\mathrm{ss}} + \dot{e}\right|\right)\left(\dot{x}_{\mathrm{ss}} + \dot{e}\right) + \left(k_1 + k_3\left(x_{\mathrm{ss}} + e\right)^2\right)\left(x_{\mathrm{ss}} + e\right) = m_s r\omega^2 \sin\left(\omega t + \theta\right). \tag{89}$$

Since $x_{ss}$ satisfies Eq. (41) and assuming that the non-linear terms in $e$ can be neglected, Eq. (89) can be rewritten as follows:

$$m\ddot{e} + \left(k_1 + 3k_3x_0^2\right)e + \left(c_1 + 2\mathrm{c}_2\dot{x}_0 sign\left(\dot{x}_0 + \dot{e}\right)\right)\dot{e} = 0. \tag{90}$$

This differential equation governs the jump effect of the response. Substituting Eq. (42) into Eq. (90) gives:

$$m\ddot{e} + \left(k_1 + 3k_3X_1^2\sin\left(\omega t\right)^2\right)e + \left(c_1 + 2\mathrm{c}_2\omega X_1\cos\left(\omega t\right)sign\left(\omega X_1\cos\left(\omega t\right) + \dot{e}\right)\right)\dot{e} = 0, \tag{91}$$

which is a second order differential equation with variable coefficients. As pointed in Ref. [42], the solution of this differential equation is a linear combination of two independent solutions $e_1$, $e_2$, such that assuming a solution in the form [47]:

$$e(t) = A\cos\left(\omega t\right) + B\sin\left(\omega t\right), \tag{92}$$

the fundamental Fourier component of $sign\left(\omega X_1\cos(\omega t) + \dot{e}\right)$ becomes $\frac{4}{\pi}\cos(\omega t)$ [27] and thus Eq. (91) can be rearranged as follows:

$$m\ddot{e} + \left(k_1 + 3k_3X^2\sin\left(\omega t\right)^2\right)e + \left(c_1 + \frac{8}{\pi}\mathrm{c}_2\omega X\cos\left(\omega t\right)^2\right)\dot{e} = 0. \tag{93}$$

At this point, substituting Eq. (92) into Eq. (93), using the trigonometric identities and neglecting the higher order harmonics gives:

$$\left(A\left(k_1 - m\omega^2\right) + \frac{3}{4}k_3AX^2 + c_1\omega B + \frac{6}{\pi}c_2\omega^2BX\right)\cos\left(\omega t\right) + \left(B\left(k_1 - m\omega^2\right) + \frac{9}{4}k_3BX^2 - c_1\omega A - \frac{2}{\pi}c_2\omega^2AX\right)\sin\left(\omega t\right) = 0. \tag{94}$$

Equating the coefficients of $\cos(\omega t)$ and $\sin(\omega t)$ results into the following two expressions:

$$A\left(k_1 - m\omega^2\right) + \frac{3}{4}k_3AX^2 + c_1\omega B + \frac{6}{\pi}c_2\omega^2BX, \tag{95}$$

$$B\left(k_1 - m\omega^2\right) + \frac{9}{4}k_3BX^2 - c_1\omega A - \frac{2}{\pi}c_2\omega^2AX. \tag{96}$$

This set of two equations can be cast in matrix form:

$$\begin{bmatrix} k_1 - m\omega^2 + \frac{3}{4}k_3X^2 & c_1\omega + \frac{6}{\pi}c_2\omega^2X \\ -c_1\omega - \frac{2}{\pi}c_2\omega^2X & k_1 - m\omega^2 + \frac{9}{4}k_3X^2 \end{bmatrix}\begin{bmatrix} A \\ B \end{bmatrix} = \begin{bmatrix} 0 \\ 0 \end{bmatrix} \tag{97}$$

Non-trivial solutions are found by setting the determinant of this matrix to zero, which gives:

$$\frac{27}{16}k_3^2X^4 + \left(3k_3\left(k_1 - m\omega^2\right) + \frac{12}{\pi^2}c_2^2\omega^4\right)X^2 + \frac{8}{\pi}c_1c_2\omega^3X + \left(k_1 - m\omega^2\right)^2 + c_1^2\omega^2 = 0. \tag{98}$$

The area between the two positive loci of Eq. (98) identifies the instability region of the steady-state harmonic motion of the system governed by Eq. (41). It is interesting to note that under the assumption of small unbalance mass i.e. $m_s \ll m_m$ and for fixed stiffness and damping parameters, Eq. (98) is invariant under changes of the unbalance amplitude of excitation $m_s r\omega^2$. The common solutions between Eqs. (98) and Eq. (41) give the two critical points of the system, which correspond to the vertical tangents of the spectrum [41–44]. Figure 17 shows that, for different

values of the unbalance mass $m_s$, the stability curve intersects the frequency response at the two vertical slopes, which defines the region of instability. As expected, as the value of the unbalance mass is increased, the region of instability increases.

**Author Contributions** LDB, PG, NB and ET: conceptualization, investigation, writing—review and editing.

**Funding** Open access funding provided by Università degli Studi di Udine within the CRUI-CARE Agreement. The authors received no financial support for the research, authorship, and/or publication of this article.

**Availability of Data and Materials** None.

**Code Availability** None.

## Declarations

**Conflict of Interest** The authors declared no potential conflict of interest with respect to the research, authorship, and/or publication of this article.

**Ethics Approval** Not relevant.

**Consent to Participate** Not relevant.

**Consent for Publication** Not relevant.



## References

1. Friswell MI, Penny JET, Garvey SD, Lees AW (2015) Dynamics of rotating machines. University Press, Cambridge
2. Muszynska A (2005) Rotordynamics. CRC Taylor & Francis Group, New York
3. Adams ML (2010) Rotating machinery vibration : from analysis to troubleshooting. CRC Press/Taylor & Francis, Boca Raton
4. Genta G (2005) Dynamics of rotating systems. Springer, New York
5. Genta G (1999) Vibration of structures and machines: practical aspects. Springer, New York
6. Sève F, Andrianoely MA, Berlioz A, Dufour R, Charreyron M (2003) Balancing of machinery with a flexible variable-speed rotor. J Sound Vib 264:287–302
7. MacCamhaoil M Static and Dynamic Balancing of Rigid Rotors. Bruel & Kjaer application notes, BO 0276–12. http://www.bksv.com/doc/BO0276.pdf
8. Rivin EI (2001) Passive vibration isolation. ASME Press, New York
9. Snowdon JC (1979) Vibration isolation: use and characterization. J Acoust Soc Am 66:1245–1274
10. Zhang F, Shao S, Tian XuM, Xie S (2019) Active-passive hybrid vibration isolation with magnetic negative stiffness isolator based on Maxwell normal stress. Mech Syst Signal Process 123:244–263
11. Daley S, Hätönen J, Owens DH (2005) Active vibration isolation in a "Smart Spring" mount using a repetitive control approach. IFAC Proc 38:55–60
12. Gardonio P, Elliott SJ (1999) A study of control strategies for the reduction of structural vibration transmission. J Vib Acous Trans ASME 121:482–487
13. Gardonio P, Elliott SJ (2000) Passive and active isolation of structural vibration transmission between two plates connected by a set of mounts. J Sound Vib 237:483–511
14. Krysinski T, Malburet F (2010) Mechanical vibrations: active and passive control. Wiley-ISTE, London
15. Ho C, Lang ZQ, Billings SA (2014) Design of vibration isolators by exploiting the beneficial effects of stiffness and damping nonlinearities. J Sound Vib 333:2489–2504
16. Lee CM, Goverdovskiy VN, Temnikov AI (2007) Design of springs with "negative" stiffness to improve vehicle driver vibration isolation. J Sound Vib 302:865–874
17. Carrella A, Friswell MI, Zotov A, Ewins DJ, Tichonov A (2009) Using non-linear springs to reduce the whirling of a rotating shaft. Mech Syst Signal Process 23:2228–2235
18. Spelta C, Previdi F, Savaresi SM, Fraternale G, Gaudiano N (2009) Control of magnetorheological dampers for vibration reduction in a washing machine. Mechatronics 19:410–421
19. Carrella A, Brennan MJ, Waters TP (2007) Static analysis of a passive vibration isolator with quasi-zero-stiffness characteristic. J Sound Vib 301:678–689
20. Carrella A, Brennan MJ, Waters TP, Lopes V (2012) Force and displacement transmissibility of a nonlinear isolator with high-static-low-dynamic-stiffness. Int J Mech Sci 55:22–29
21. Tang B, Brennan MJ (2013) A comparison of two non-linear damping mechanisms in a vibration isolator. J Sound Vib 332:510–520
22. Lang ZQ, Jing XJ, Billings SA, Tomlinson GR, Peng ZK (2009) Theoretical study of the effects of non-linear viscous damping on vibration isolation of sdof systems. J Sound Vib 323:352–365
23. Lv Q, Yao Z (2015) Analysis of the effects of non-linear viscous damping on vibration isolator. Non-linear Dyn 79:2325–2332
24. Peng ZK, Meng G, Lang ZQ, Zhang WM, Chu FL (2012) Study of the effects of cubic non-linear damping on vibration isolations using Harmonic Balance Method. Int J Non Linear Mech 47:1073–1080
25. Ravindra B, Mallik AK (1993) Hard duffing-type vibration isolator with combined Coulomb and viscous damping. Int J Non Linear Mech 28:427–440
26. Zhang B, Billings SA, Lang ZQ, Tomlinson GR (2009) Suppressing resonant vibrations using nonlinear spring and dampers. J Vib Control 1:1–14
27. Elliott SJ, Tehrani MG, Langley RS (2015) Non-linear damping and quasi-linear modelling. Phil Trans R Soc A Math Phys Eng Sci 373:20140402
28. Mallik AK, Kher V, Puri M, Hatwal H (1999) On the modelling of non-linear elastomeric vibration isolators. J Sound Vib 219:239–253
29. Ravindra B, Mallik AK (1994) Performance of non-linear vibration isolators under harmonic excitation. J Sound Vib 170:325–337

30. Sun X, Jing X (2016) A nonlinear vibration isolator achieving high-static–low-dynamic stiffness and tunable anti-resonance frequency band. Mech Syst Signal Process 80:166–188
31. Lu Z et al (2013) An investigation of a two-stage nonlinear vibration isolation system. J Sound Vib 332(6):1456–1464
32. Balaji PS, Karthik SelvaKumar K (2021) Applications of nonlinearity in passive vibration control: a review. J Vib Eng Technol 9:183–213
33. Van Engelen NC (2019) Fiber-reinforced elastomeric isolators: a review. Soil Dyn Earthq Eng 125:105621
34. andasamy R, et al (2016) A review of vibration control methods for marine offshore structures. Ocean Eng 127:279–297
35. Ibrahim RA (2008) (2012) Recent advances in non-linear passive vibration isolators. J Sound Vib 314:371–452
36. Friswell MI (2012) Saavedra Flores EI and Xia Y. Vibration isolation using non-linear springs. In: Sas P, Moens D, Jonckheere S (eds) Proc. of ISMA-USD 2012, Leuven, Belgium, 17 – 19 September 2012, pp 2333–2342
37. Hanna NH, Tobias SA (1974) Theory of non-linear regenerative chatter. J Eng Ind 96:247–255
38. Jiang W, Zhang G, Chen L (2015) Forced response of quadratic non-linear oscillator: comparison of various approaches. Appl Math Mech 36:1403–1416
39. Virgin LN (1988) On the harmonic response of an oscillator with unsymmetric restoring force. J Sound Vib 126:157–165
40. Hanna NH, Tobias SA (1969) The non-linear dynamic behaviour of a machine tool structure. Int J Mach Tool Des Res 9:293–307
41. Stoker JJ (1992) Non-linear vibrations in mechanical and electrical systems. John Wiley & Sons, New York
42. Nayfeh AH, Mook DT (1979) Non-linear oscillations. Wiley-Interscience, New York
43. Dominic DW, Jordan W, Smith P (2007) Non-linear ordinary differential equations: an introduction for scientists and engineers. Oxford University Press, Oxford
44. Hayashi C (1964) Non-linear oscillations in physical systems. McGraw-Hill, New York
45. Malatkar P, Nayfeh AH (2002) Calculation of the jump frequencies in the response of s.d.o.f. non-linear systems. J Sound Vib 254:1005–1011
46. Nayfeh AH, Balachandran B (1995) Applied nonlinear dynamics, 1st edn. Wiley, New York
47. Jazar GN, Houim R, Narimani A, Golnaraghi MF (2006) Frequency response and jump avoidance in a non-linear passive engine mount. J Vib Control 12:1205–1237
48. Worden K (1996) On jump frequencies in the response of the Duffing oscillator. J Sound Vib 198:522–525